JOURNAL OF COMPUTATIONAL PHYSICS 56, 363–409 (1984)

Review Article

Two-Phase Flow: Models and Methods

H. BRUCE STEWART

Applied Mathematics Department, Brookhaven National Laboratory, Upton, New York 11937

AND

BURTON WENDROFF

Theoretical Division, Los Alamos National Laboratory, Los Alamos, New Mexico 87544

Received August 5, 1983; revised March 30, 1984

A variety of two-phase flow models can be derived following a few basic principles, which are here illustrated which no more generality than is essential. Among the models derived is one already widely used in applications, even though it is ill-posed in the sense of Hadamard. Final assessment of such models remains a distant goal, but will clearly involve numerical solutions; several methods in current use are discussed with a guide to selecting the one appropriate to a particular problem.

CONTENTS. I. *Models.* 1.0. Preface. 1.1. An Example of a Multifield Flow. 1.2. The Local Description. 1.3. Averaging. 1.4. Nonequilibrium Models. 2.0. Noninteracting Fields. 2.1. One-dimensional Stratified Flow. 2.2. Three-dimensional Irregular Flow. 2.3. The Basic Model. 2.4. Other Models. 3.0. Interacting Fields. 3.1. Mass Transfer Effects. 3.2. Mutual Forces. 3.3. Viscosity, Surface Tension, and Heat Conduction. 3.4. Practical Limitations. 4.0. Limiting Cases. 4.1. Equal Velocities. 4.2. Asymptotics and the Drift Flux Approximation. 4.3. Homogeneous Equilibrium. II. *Methods.* 5.0. Theoretical Considerations for Numerical Methods. 5.1. Scales. 5.2. Stability. 6.0. Eulerian Finite Difference Methods. 6.1. The Grid. 6.2. Semi-implicit Schemes. 6.3. Fully Implicit Schemes. 6.4. Explicit Schemes. 7.0. Other Methods. 7.1. Method of Characteristics. 7.2. Lagrangian Methods. 7.3. Weighted Residuals. Appendix 1.

I. MODELS

1.0. *Preface*

The type of multiphase flow we will concentrate on in this survey typically consists of a mixture of water and air or of water and steam. Since we will allow the water to

0021-9991/84 $3.00

be compressible we might just as well from the start discuss the dynamics of a mixture of two compressible fluids, where fluid now means either liquid or gas. In that case it is better to adopt terminology proposed by Harlow [67] and use the word *field* rather than fluid. We are thereby not necessarily restricted to liquids and gases; our models and methods might (and often will) apply to mixtures of solids, liquids, and gases, or even to more esoteric situations in which one field might consist of the laminar portion of a flow, the other the turbulent portion. The models we survey are notable for treating the fields as interpenetrating; that is, each has its own velocity vector field, and in the interesting flow region both velocity fields exist at every point. We are not, however, trying to present a general theory of mixtures; our fields are not mixing on a molecular level, as would two gases. At any time the spatial region occupied by field 1 in reality is disjoint from the region occupied by field 2. Interpenetration arises by way of an approximation on a scale coarser than the molecular; we will discuss this in detail.

1.1. *An Example of a Multifield Flow*

The example we are most familiar with occurs in conventional nuclear reactors cooled by water under pressure. Such a reactor consists of a heat producing core and a system of pipes, pumps, accumulators, and heat exchangers through which, under normal operating conditions, there is a flow of mostly liquid water. Note that the complicated geometry makes this single field problem already nontrivial. If a large break occurs in a pipe there will be a sudden depressurization and the water will begin to turn to steam. Figures 1.1 to 1.4 show a variety of steam–water configurations that can occur as the pressure in the system drops.

The presence of such topologically complicated interfaces, and the transitions from one type to another, suggest the need for a multifield model of the flow.

1.2. *The Local Description*

Suppose there are two fields which in reality occupy disjoint time-dependent domains $\Omega_i(t)$, $i = 1, 2$. There will be two systems of partial differential equations describing the state of the fields, each system being valid in one of the Ω_i. Thus, we may write

$$\frac{\partial w_i(x, t)}{\partial t} = \mathscr{L}_i(w_i), \qquad \text{for } x \text{ in } \Omega_i, x = (x_1, x_2, x_3), \tag{1.2.1}$$

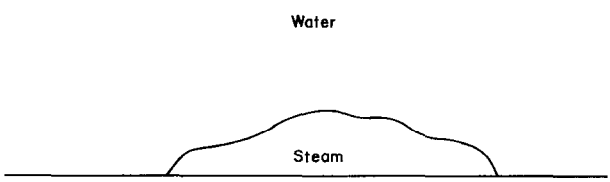

FIG. 1.1. Simple phase front.

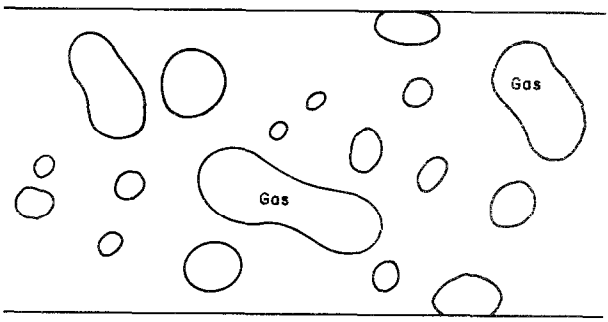

FIG. 1.2. Bubbly mixture.

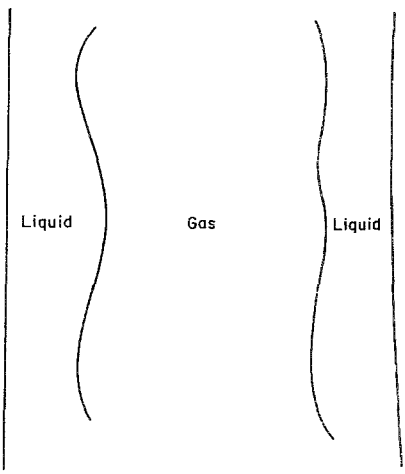

FIG. 1.3. Annular flow.

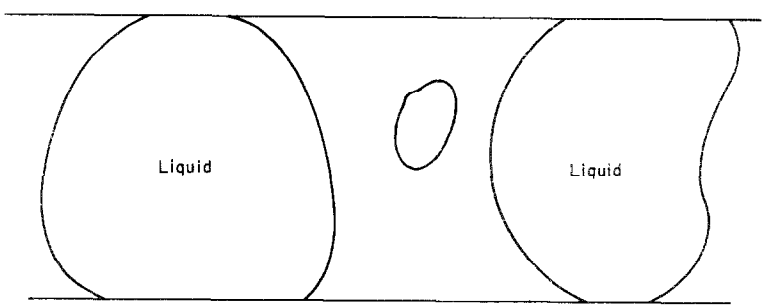

FIG. 1.4. Slugs, etc.

where w_i is the state vector of the ith field, and $\mathscr{L}_i$ is an appropriate partial differential operator. For example, if each field were inviscid these would just be the Euler equations.

Additional conditions must be imposed in order to have any chance that a given initial state will evolve in time in a unique way. First, if

$$\Omega = \Omega_1 \cup \Omega_2,$$

and

$$\partial\Omega := \text{boundary of } \Omega,$$

then boundary conditions must be imposed on $\partial\Omega$. Second, conditions must be posed on the separating interface, that is, on

$$S(t) = (\partial\Omega_1 \cup \partial\Omega_2)/\partial\Omega.$$

BASIC ASSUMPTION. *We will assume that Eq.* (1.2.1) *together with the initial data and boundary and interface conditions uniquely determines the state vectors* $w_i(x, t)$ *and the domains* $\Omega_i(t)$, *within some class of physically correct solutions.*

The collection of differential equations and extra conditions is called the *complete local description* of the flow. Clearly, except in very special circumstances, it is impossible to compute the flow using the local description. It is necessary to resort to models which suppress some details of the flow, but are computable. Although this can sometimes be done using physical first principles, it has long been recognized [1–5], that averaging of the complete local description provides a rational procedure for deriving models.

1.3. *Averaging*

The standard reference on averaging as a means of obtaining practical models of multifield flow is Ishii [1]. Ishii concentrates on time averaging, but he discusses and provides references to spatial and statistical averaging; [65, 66, 68] are also excellent sources. In Section 2 we give some detailed examples of averaging; here we only sketch the basic idea.

We begin by supposing that the state vectors w_i depend on some vector parameter r (which could involve the space and time variables). This parameter varies over some set R_i which may depend on x and t. Thus,

$$w_i = w_i(x, t, r), \qquad r \text{ in } R_i(x, t).$$

We want to replace the point functions w_i by integrals over the R_i. Thus, we suppose that integration is defined over R_i; let

$$\mathscr{A}_i = \int_{R_i(x,t)} dr.$$

Applying $\mathscr{A}_i$ to Eq. (1.2.1), we wish to consider

$$\partial_t \mathscr{A}_i w_i = \mathscr{L}_i(\mathscr{A}_i w_i) + C_i,$$

where $\partial_t = \partial/\partial t$, and

$$C_i = [\partial_t \mathscr{A}_i w_i - \mathscr{L}_i(\mathscr{A}_i w_i)] - \mathscr{A}_i[\partial_t w_i - \mathscr{L}_i(w_i)].$$

The commutator C_i depends on averages, local quantities, boundary values, and interfacial values. To close the system C_i must be replaced by someting which depends only on averages and interface descriptors. When this is done the following general system will result:

$$\begin{aligned} \partial_t \phi_i &= \mathscr{L}_i(\phi_i) + \mathscr{C}_i(\phi_1, \phi_2, \sigma_1, \ldots, \sigma_n), \\ \partial_t \sigma_j &= \mathscr{M}_j(\phi_1, \phi_2, \sigma_1, \ldots, \sigma_n), \qquad j = 1, n, \end{aligned} \tag{1.3.1}$$

plus boundary conditions. The ϕ_i represent the averages, while the σ_j are the interface descriptors. $\mathscr{C}_i$ and $\mathscr{M}_j$ are differential operators which couple the averaged fields. These operators should be chosen so that the usual total conservation laws are satisfied by the averages.

1.4. *Nonequilibrium Models*

Except in the special case of a completely homogeneous mixture, multifield flow is intrinsically a nonequilibrium process. Although we will always assume that each field is in local thermodynamic equilibrium, the different fields are not in equilibrium with each other. The reader familiar with nonequilibrium gas dynamics will see that the σ_j play the role of nonequilibrium parameters obeying certain rate equations (see [6]). In our case we must supply rates of transfer of momentum, mass, and energy from one phase to the other, in order to close the rate equations. These must usually be obtained from empirical data, and they are a major source of error.

2.0. *Noninteracting Fields*

In this chapter we amplify the abstract discussion of averaging given in Subsection 1.3. The first example is the reduction of 2-dimensional stratified flow to one dimension, which is very closely related to the area-averaged 1-dimensional flow of a gas in a variable area duct. We do this in great detail, with a statement of all the closure assumptions that are made in order to have the number of unknown functions be the same as the number of equations. With the minimal number of such assumptions we obtain a rather large and unwieldy system of partial differential equations: this system is *not* offered as a practical model but only as an illustration of the full averaging procedure and of the difficulties caused by allowing the two fields to have different velocities. To do this in complete detail for multidimensional flows with a complicated interface would require as much space as Ishii's book; instead, we will try to convince the reader that our example is already decisive for the

general form of the averaged equations, with further differences occuring only in the coupling operators $\mathscr{C}_i, \mathscr{M}_j$ of Subsection 1.3.

2.1. *One-dimensional Stratified Flow*

The flow to be considered here consists of two inviscid fields between parallel flat plates, separated by a smooth single-valued surface, as shown in Fig. 2.1.

The flow is assumed to depend only on the longitudinal variable x and the axial variable y, and time. Heat conduction, external forces, and transfer of mass, momentum, and energy between fields are assumed to be absent. This is described by eight local field equations,

$$\partial_t \tilde{\rho}_i + \partial_x(\tilde{\rho}_i \tilde{u}_i) + \partial_y(\tilde{\rho}_i \tilde{v}_i) = 0, \tag{2.1.1}$$

$$\partial_t(\tilde{\rho}_i \tilde{u}_i) + \partial_x(\tilde{\rho}_i \tilde{u}_i^2 + \tilde{p}_i) + \partial_y(\tilde{\rho}_i \tilde{u}_i \tilde{v}_i) = 0, \tag{2.1.2}$$

$$\partial_t(\tilde{\rho}_i \tilde{v}_i) + \partial_x(\tilde{\rho}_i \tilde{u}_i \tilde{v}_i) + \partial_y(\tilde{\rho}_i \tilde{v}_i^2 + \tilde{p}_i) = 0, \tag{2.1.3}$$

$$\partial_t(\tilde{\rho}_i \tilde{S}_i) + \partial_x(\tilde{\rho}_i \tilde{u}_i \tilde{S}_i) + \partial_y(\tilde{\rho}_i \tilde{v}_i \tilde{S}_i) = 0, \tag{2.1.4}$$

where $\tilde{\rho}_i = \tilde{\rho}_i(x, y, t)$ are the local densities, $\tilde{u}_i$ and $\tilde{v}_i$ are the longitudinal and transverse velocities, $\tilde{p}_i$ the pressures, and $\tilde{S}_i$ the entropies of each field. For $i = 1$ the equations hold for $0 < y < d\alpha(x, t)$, while for $i = 2$, $\alpha d < y < d$. In addition, there is an equation of state for each field, $\tilde{p}_i = \tilde{p}_i(\tilde{\rho}_i, \tilde{S}_i)$, and the temperature $\tilde{T}_i$ and internal energies $\tilde{e}_i$ satisfy $\tilde{T}_i \, d\tilde{S}_i = d\tilde{e}_i + \tilde{p}_i d(\tilde{\rho}_i)$.

The averaging operators are

$$\mathscr{A}_i = \int_{a_{i-1}}^{a_i} dy, \qquad i = 1, 2,$$

where $a_0 = 0$, $a_1 = \alpha d$, $a_2 = d$. Let ∂ stand for ∂_t or ∂_x. Then for any smooth functions $a(x, t)$, $b(x, t)$,

$$\int_{a(x,t)}^{b(x,t)} \partial f \, dy = \partial \int_{a(x,t)}^{b(x,t)} f \, dy - [f(x, b, t) \, \partial b - f(x, a, t) \, \partial a]. \tag{2.1.5}$$

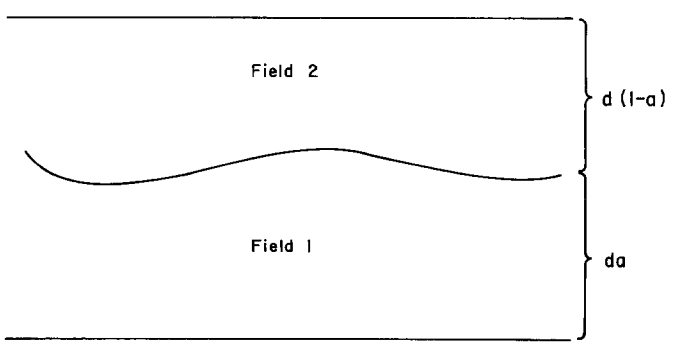

FIG. 2.1. Stratified flow.

We adopt the following notation:

$$f_i := \frac{1}{a_i - a_{i-1}} \mathscr{A}_i \tilde{f}_i,$$

$$\hat{f}_i = \lim_{y \to \alpha} \tilde{f}_i(x, y, t),$$

$$\tilde{f}^0 = \tilde{f}_1(x, 0, t),$$

$$\tilde{f}^d = \tilde{f}_2(x, d, t),$$

$$\alpha_1 = \alpha,$$

$$\alpha_2 = 1 - \alpha_1.$$

Then applying $\mathscr{A}_i$ to the ith equation of (2.1.1) and using (2.1.5) produces

$$\partial_t(\alpha_1 \rho_1) + \partial_x(\alpha_1(\rho u)_1) = \hat{p}_1 \left[\partial_t \alpha_1 + \hat{u}_1 \partial_x \alpha_1 - \frac{\hat{v}_1}{d} \right] + \frac{\tilde{\rho}^0 \tilde{v}^0}{d},$$

$$\partial_t(\alpha_2 \rho_2) + \partial_x(\alpha_2(\rho u)_2) = \hat{p}_2 \left[\frac{\hat{v}_2}{d} - (\partial_t \alpha_1 + \hat{u}_2 \partial_x \alpha_1) \right] - \frac{\tilde{\rho}^d \tilde{v}^d}{d}.$$

The following boundary and interface conditions are imposed:

Boundary Condition BC1 (normal component of velocity zero at the horizontal boundaries),

$$\tilde{v}^0 = \tilde{v}^d = 0. \tag{2.1.6}$$

Interface Condition IC1 (streamlines form interface),

$$\partial_t \alpha_1 + \hat{u}_1 \partial_x \alpha_1 - \frac{\hat{v}_1}{d} = 0, \tag{2.1.7}$$

$$\partial_t \alpha_1 + \hat{u}_2 \partial_x \alpha_1 - \frac{\hat{v}_2}{d} = 0. \tag{2.1.8}$$

With these conditions (2.1.1) becomes

$$\partial_t(\alpha_i \rho_i) + \partial_x(\alpha_i(\rho u)_i) = 0, \tag{2.1.9}$$

expressing the conservation of mass of each field.

Going through the same operation for (2.1.2) leads to

$$\partial_t(\alpha_1(\rho u)_1) + \partial_x[\alpha_1((\rho u^2)_1 + p_1)] = \hat{p}_1 \partial_x \alpha_1$$

and

$$\partial_t(\alpha_2(\rho u)_2) + \partial_x[\alpha_2((\rho u^2)_2 + p_2)] = -\hat{p}_2 \partial_x \alpha_1.$$

The total longitudinal momentum will satisfy a conservation law if

Interface Condition IC2,

$$\hat{p}_1 = \hat{p}_2 := \hat{p}, \tag{2.1.10}$$

in which case (2.1.2) becomes

$$\partial_t(\alpha_i(\rho u)_i) + \partial_x[\alpha_i((\rho u^2)_i + p_i)] = \hat{p}\partial_x\alpha_i. \tag{2.1.11}$$

The entropy equation (2.1.4) goes into

$$\partial_t(\alpha_i(\rho S)_i) + \partial_x(\alpha_i(\rho u S)_i) = 0. \tag{2.1.12}$$

The transverse momentum equation becomes

$$\partial_t(\alpha_1(v\rho)_1) + \partial_x(\alpha_1(\rho uv)_1) = (\tilde{p}^0 - \hat{p})/d,$$
$$\partial_t(\alpha_2(v\rho)_2) + \partial_x(\alpha_2(\rho uv)_2) = (\hat{p} - \tilde{p}^d)/d.$$

To get rid of $\tilde{p}^0$ and $\tilde{p}^d$, we have

Boundary Condition BC2 (rigid boundaries in terms of average pressures),

$$\tilde{p}^0 = p_1, \qquad \tilde{p}^d = p_2,$$

so

$$\partial_t(\alpha_i(\rho v)_i) + \partial_x(\alpha_i(\rho uv)_i) = (-1)^i(\hat{p} - p_i)/d. \tag{2.1.13}$$

Neither (2.1.3) nor (2.1.13) appear to conserve total transverse momentum, but symmetric extension into $d < y < 2d$ conserves total momentum in $0 < y < 2d$ without changing the solution in $0 < y < d$.

We have not really introduced any approximations up to this point, but the time has come since we have many more unknown functions than equations. We make the following standard closure assumptions, which are motivated not by physics but by the need to have a tractable model:

$$u_i := \frac{(\rho u)_i}{\rho_i},$$
$$(\rho u^2)_i := \rho_i u_i^2,$$
$$(\rho S)_i := \rho_i S_i,$$
$$(\rho u S)_i := \rho_i u_i S_i.$$

We also need an equation of state for the average pressure p_i. We have little choice but to set

$$p_i = \tilde{p}_i(\rho_i, S_i),$$
$$e_i = \tilde{e}_i(\rho_i, S_i),$$

and

$$T_i = \tilde{T}_i(\rho_i, S_i),$$

so that

$$T_i\, dS_i = de_i + p_i\, d(1/\rho_i). \tag{2.1.14}$$

We can now derive total energy transport equations. For the internal energy we have

$$\partial_t(\rho_i\alpha_i e_i) + \partial_x(\rho_i\alpha_i u_i e_i) + p_i[\partial_t\alpha_i + \partial_x(\alpha_i u_i)] = 0.$$

For the longitudinal contribution to the kinetic energy the equation is

$$\partial_t(\alpha_i\rho_i\tfrac{1}{2}u_i^2) + \partial_x(u_i\alpha_i\tfrac{1}{2}u_i^2) + u_i\partial_x(\alpha_i p_i) - u_i\hat{p}_i\partial_x\alpha_i = 0.$$

The transverse contribution is

$$\partial_t(\alpha_i\rho_i\tfrac{1}{2}v_i^2) + \partial_x(u_i\alpha_i\rho_i\tfrac{1}{2}v_i^2) - v_i(-1)^i\,((\hat{p} - p_i)/d) = 0.$$

Then

$$\sum_{i=1}^{2} \partial_t[\rho_i\alpha_i(e_i + \tfrac{1}{2}u_i^2 + \tfrac{1}{2}v_i^2)] + \partial_x[u_i\rho_i\alpha_i(e_i + \tfrac{1}{2}u_i^2 + \tfrac{1}{2}v_i^2) + \alpha_i u_i p_i]$$
$$+ p_i\partial_t\alpha_i + u_i p_i\partial_x\alpha_i - u_i\hat{p}\partial_x\alpha_i - v_i(-1)^i\,((\hat{p} - p_i)/d) = 0.$$

This becomes a conservation law if

$$(p_1 - p_2)\,\partial_t\alpha_1 + [u_1 p_1 - u_2 p_2 - \hat{p}(u_1 - u_2)]\,\partial_x\alpha_1$$
$$- \sum_{i=1}^{2} v_i(-1)^i\left(\frac{\hat{p} - p_i}{d}\right) = 0. \tag{2.1.15}$$

There is only one *simple* way to use this, and that is to adopt

Interface Condition IC3,

$$\hat{v}_i = v_i, \qquad i = 1, 2. \tag{2.1.16}$$

Then using (1.1.7), (2.1.8) in (2.1.15) we obtain

$$(\partial_x\alpha_1)[u_1 p_1 - u_2 p_2 - \hat{p}(u_1 - u_2) + \hat{u}_1(\hat{p} - p_1) - \hat{u}_2(\hat{p} - p_2)] = 0. \tag{2.1.17}$$

Among the infinitely many ways of satisfying (2.1.17), three seem particularly attractive.

System A: $\hat{u}_1 = u_1, \hat{u}_2 = u_2$.

There are now the eight field equations (2.1.9), (2.1.11), (2.1.12), (2.1.13) and the two interfacial transport equations (2.1.7), (2.1.8), or 10 equations. But there are also

10 unknowns, namely, $\rho_1, \rho_2, u_1, u_2, v_1, v_2, S_1, S_2, \alpha, \hat{p}$. Notice that everything but $\hat{p}$ can be advanced in time by a partial differential equation. If we replace (2.1.8) by the compatibility condition

$$(u_2 - u_1)\,\partial_x \alpha = (v_2 - v_1)/d,$$

then it is that condition which has to determine $\hat{p}$. System A seems to be new; it would be very difficult to solve numerically.

System B: $\hat{u}_1 = \hat{u}_2 = (u_1 + u_2)/2, \qquad \hat{p} = (p_1 + p_2)/2.$

Now there are 10 equations, but 9 unknowns. This can be fixed by setting $v_2 = v_1 = v$. Now (2.1.8) is superfluous, and if we add together the two transverse momentum equations (which does not affect the energy balance) there are eight unknowns and eight equations, namely (2.1.9), (2.1.11), (2.1.12), (2.1.7), and

$$\partial_t[(\alpha_1\rho_1 + \alpha_2\rho_2)\,v] + \partial_x[(\alpha_1\rho_1 u_1 + \alpha_2\rho_2 u_2)\,v] = -\,((p_1 - p_2)/d). \tag{2.1.18}$$

This is a very interesting system which was discovered in 1976 by Ransom and Schofield [7], who also did some numerical experiments comparing System B with System C, obtaining comparable results. The report by Ransom and Schofield was not widely circulated, so System B has not received much attention. A recent paper by Ransom and Hicks [18] is based on the earlier report.

System C: $\hat{p} = p_1 = p_2.$

There are too many equations, and the only sensible ones to drop are the two interfacial transport equations and the two transverse momentum equations. This leaves *six* equations,

$$\partial_t(\alpha_i\rho_i) + \partial_x(\alpha_i\rho_i u_i) = 0, \tag{2.1.19}$$

$$\partial_t(\alpha_i\rho_i u_i) + \partial_x(\alpha_i\rho_i u_i^2) + \alpha_i\partial_x p = 0, \tag{2.1.20}$$

$$\partial_t(\alpha_i\rho_i S_i) + \partial_x(\alpha_i\rho_i S_i) = 0. \tag{2.1.21}$$

This is the basic equal pressure model, which, in spite of mathematical difficulties to be discussed in Section 2.3, is the basis of the successful TRAC code [8].

2.2. *Three-dimensional Irregular Flow*

The extension of the simple example of the previous section to other types of averaging for irregular 3-dimensional flows is not trivial, but it does not differ in principle from that example. One obtains mass, momentum, and energy equations as follows:

$$\partial_t(\alpha_i\rho_i) + \nabla\cdot(\alpha_i\rho_i\mathbf{v}_i) = 0, \tag{2.2.1}$$

$$\partial_t(\alpha_i\rho_i\mathbf{v}_i) + \nabla\cdot(\alpha_i\rho_i\mathbf{v}_i\mathbf{v}_i) + \nabla(\alpha_i p_i) = \hat{p}\nabla\alpha_i, \tag{2.2.2}$$

$$\partial_t(\alpha_i\rho_i e_i) + \nabla\cdot(\alpha_i\rho_i\mathbf{v}_i e_i) + p_i[\partial_t\alpha_i + \nabla\cdot(\alpha_i\mathbf{v}_i)] = 0 \tag{2.2.3}$$

(α_i is the volume fraction of the ith field; $\mathbf{v}_i$ is its velocity).

System C is obtained by setting $\hat{p} = p_i = p$. System B can be generalized by setting $\hat{p} = \frac{1}{2}(p_1 + p_2)$ and then setting $\mathbf{w} = \frac{1}{2}(\mathbf{v}_1 + \mathbf{v}_2)$ in the α-transport equation

$$\partial_t \alpha_1 + \mathbf{w} \cdot \nabla \alpha_1 = 0. \tag{2.2.4}$$

Yet another possibility has been suggested by Harlow and Holm. Associate a mass density M moving with the surface such that

$$M(\partial_t \mathbf{w} + \mathbf{w} \cdot \nabla \mathbf{w}) = (p_2 - p_1) \nabla \alpha_1 \tag{2.2.5}$$

and

$$\partial_t M + \nabla \cdot \mathbf{w} M = 0. \tag{2.2.6}$$

In addition, drop interface condition IC2 (Eq. 2.1.10), using instead $\hat{p}_1 = p_1$, $\hat{p}_2 = p_2$. Then Eq. (2.2.2) becomes

$$\partial_t(\alpha_i \rho_i \mathbf{v}_i) + \nabla \cdot (\alpha_i \rho_i \mathbf{v}_i \mathbf{v}_i) + \alpha_i \nabla p_i = 0. \tag{2.2.7}$$

The full system (2.2.1), (2.2.7), (2.2.3), (2.2.4), (2.2.5), and (2.2.6) conserves momentum and energy provided we include $M\mathbf{w}$ in the former and $\frac{1}{2}M|w|^2$ in the latter.

Note that formally passing to the limit $M = 0$ produces $p_1 = p_2$. The relation between this model and others would be worthy of further study.

2.3. *The Basic Model*

The main purpose of Subsections 2.1 and 2.2 has been to illustrate the averaging procedure. It is, in fact, a rather subtle process which is certainly deserving of the detailed attention given to it in [1 and 3]. Rather than attempt additional development of these ideas, we are going to simply accept the basic equal pressure model and its extension to three dimensions. Let $\mathbf{v}_i$ = velocity vector of ith field. Then

$$\begin{aligned} \partial_t(\alpha_i \rho_i) + \nabla \cdot (\alpha_i \rho_i \mathbf{v}_i) &= 0, \\ \partial_t(\alpha_i \rho_i \mathbf{v}_i) + \nabla \cdot (\alpha_i \rho_i \mathbf{v}_i \mathbf{v}_i) + \alpha_i \nabla p &= 0, \end{aligned} \tag{2.3.1}$$

and either

$$\partial_t(\alpha_i \rho_i S_i) + \nabla \cdot (\alpha_i \rho_i S_i \mathbf{v}_i) = 0,$$

or

$$\partial_t(\alpha_i \rho_i e_i) + \nabla \cdot (\alpha_i \rho_i e_i \mathbf{v}_i) + p[\partial_t(\alpha_i) + \nabla \cdot (\alpha_i \mathbf{v}_i)] = 0,$$

or

$$\partial_t(\alpha_i \rho_i E_i) + \nabla \cdot (\alpha_i(\rho_i E_i + p)\, \mathbf{v}_i) + p \partial_t(\alpha_i) = 0.$$

where

$$E_i = e_i + \tfrac{1}{2}\mathbf{v}_i \cdot \mathbf{v}_i.$$

Note that the momentum and total energy equations of the individual fields are *not* in conservation form.

Under the assumption of equal pressures, these are the equations that one arrives at by averaging, whether it be time, space, or statistical. The complicated interface between the fields, as would exist, for example, in bubbly flow, is entirely absorbed into the quantity α_i, which is now no longer the height but is the volume fraction of the ith field. This is the basic model which, although derived in a physically reasonable way, suffers from a serious mathematical difficulty: the system of partial differential equations is ill-posed in the sense of Hadamard [9]. More precisely, if we write the system in the form $\partial_t u + A\partial_x u = 0$, then the matrix A has a pair of complex eigenvalues in the physically interesting region of state space. This is proved in Appendix 1, although it has been known for a long time. The physical basis for this was already perceived in [10], but it is discussed in the present context in [11, 12]. This means that the solutions probably do not depend continuously on the initial data, at least not in any of the function spaces commonly used in the theory of partial differential equations. This is proved for linear equations in [13]. For nonlinear systems of the type being considered here, Lax [14] proved the nonexistence of a bounded integral of the solution unless the eigenvalues of A are real, which is pretty strong evidence that continuous dependence is lacking for our nonlinear system.

Problems which are ill-posed are difficult, but not hopeless. However, certain compromises have to be made: regularizing terms may be added to the equations, the initial data may have to be restricted to subsets of function space, or it may be necessary to use some notion of generalized solution. An example of this is the backward heat equation, on which there is a large literature [15]. A more naive example would be any process which leads to a divergent infinite series

$$\sum_{i=0}^{\infty} a_i \lambda^{-i}, \qquad \text{with the property that} \qquad \sum_{i=0}^{N} a_i \lambda^{-i}$$

is accurate for fixed N and λ sufficiently large. A practical example of an ill-posed problem can be found in geophysics, wherein one needs to solve the inverse problem of determining properties under the earth's surface from seismic data.

There are three facts that might contribute to a mathematical foundation for the basic model. The first is that the matrix A has two real genuinely nonlinear eigenvalues (in the sense of Lax [16]) which give the system wave pressure propagation properties analogous to those of gas dynamics. The second concerns something left out of the model, namely viscosity. With the inclusion of any nonzero viscosity, no matter how small, the basic model becomes well-posed in the sense that for the linearized frozen coefficient problem, perturbations of wave number k are bounded as $k \to \infty$, for any fixed time. This is shown rigorously in [17, Eqs. (61a, 61b)], where for a perturbation with space time dependence $\exp[i(\lambda t + kx)]$ the dispersion relation is shown to be the following (in the case $\rho_i = \rho_i(p)$). There are four values of $\lambda(k)$, two of them have the form

$$\lambda_b = Ak + iB + O\left(\frac{1}{k}\right), \qquad A \text{ and } B \text{ real}, \; B \geqslant 0,$$

and two of them have the form

$$\lambda_d = ia^2k^2 + O(k),$$

where $a^2 > 0$ is proportional to one of the viscosity coefficients. Then

$$\begin{aligned} |e^{i\lambda_b t}| &< \text{constant}, && k \to \infty, \\ |e^{i\lambda_d t}| &< e^{-a^2k^2t}e^{ckt}, && c \text{ some constant} > 0, \\ &\to 0 && \text{as } k \to \infty, t \text{ fixed}. \end{aligned}$$

Thus, it seems improper to consider the behavior of the differential equations at arbitrarily small wevelengths without including viscosity, which is not zero for real fluids and gases.

The third consideration is that the basic model is the formal asymptotic limit of System B (Sect. 2.1) as $d \to 0$, and System B is not ill-posed. In fact, for System B it is easy to see that the characteristic speeds are $u_1 \pm c_1, u_2 \pm c_2, \bar{u}, \bar{u}, u_1, u_2$, where c_i is the sound speed of the ith field, and $\bar{u} = (u_1 + u_2)/2$.

In spite of the above, from a strictly theoretical viewpoint the situation is still very unsatisfactory. Approximate solution makes little sense unless there is some means of establishing continuous dependence of solutions on the data. A recent step was taken in [19], where it was proved that solutions of the single pressure model do depend continuously on initial conditions if the class of solutions is restricted by certain a priori bounds. These a priori bounds arise in a natural way from the bare fact that the equations were obtained by an averaging procedure; hence the result is potentially much more general then Eq. (2.3.1). The proof does not involve linearizing the equations.

2.4. *Other Models*

Several models have been proposed which are fundamentally different from the basic model. One of these can be found in [20 and 21]. It is based on the hypothesis that there should be an equation of motion for the mixture, that is, if

$$\rho_m = \rho_1\alpha_1 + \rho_2\alpha_2$$

and

$$u_m = \frac{\rho_1\alpha_1u_1 + \rho_2\alpha_2u_2}{\rho_m},$$

then one requires

$$\rho_m(\partial_t u_m + u_m\partial_x u_m) + \partial_x p = 0, \tag{2.4.1}$$

which is *not* true for the basic model. For the latter,

$$\rho_m(\partial_t u_m + u_m\partial_x u_m) + \partial_x[\rho_1\alpha_1(u_1 - u_m)^2 + \rho\alpha_2(u_2 - u_m)^2] + \partial_x p = 0. \tag{2.4.2}$$

In order to achieve (2.4.1) the individual momentum equations are taken to be

$$\partial_t(\rho_i\alpha_i u_i) + \partial_x(\rho_i\alpha_i u_i^2) - \partial_x[\rho_i\alpha_i(u_i - u_m)^2] + \alpha_i\partial_x p = 0.$$

It is not claimed that this model applies to stratified flow, but many arguments are given to establish its validity for dispersed flow. See [31–34] for critical comments on this model.

An unequal pressure model has been proposed in [22]. The interfacial condition (2.1.10) is changed to $\hat{p}_1 = p_1, \hat{p}_2 = p_2$. Then an α-transport equation of the form $A\partial_t\alpha + B\partial_x\alpha = C$ is proposed. This transport equation renders this system well-posed.

There are other models for special situations. For example, in the flow of dusty gases the momentum equation for the dust field has no pressure gradient, and the gas field momentum equation has a pressure term with coefficient one. This is also called dilute gas-particle flow [57].

3.0. *Interacting Fields*

Noninteracting fields communicate with each other in only two ways: because they cannot occupy the same volume at the same time (i.e., $\alpha_1 + \alpha_2 = 1$), and through the pressure terms. In most applications there are more obvious mechanisms for interaction at the interface: transfer of mass through evaporation or condensation, with associated changes in momentum and energy; momentum and energy transfer due to friction; mutual forces such as surface tension and buoyancy or other stresses. In the following sections we will take up some of these issues, in as elementary and direct a way as we can.

3.1. *Mass Transfer Effects*

Suppose field 1 is steam, field 2 is water. Let Γ be the rate of production of steam mass per unit volume. Then the mass conservation equations become

$$\begin{aligned} \partial_t(\alpha_i\rho_i) + \partial_x(\alpha_i u_i\rho_i) &= \Gamma_i, \\ \Gamma_1 = \Gamma &= -\Gamma_2. \end{aligned} \tag{3.1.1}$$

The quantity Γ must be given as a function of the other variables.

The effect of mass transfer on the momentum equation is less clear. Conservation of momentum requires that the form be

$$M_1 = -M_2. \tag{3.1.2}$$

M_1 should be a velocity times Γ, but what velocity? A convenient choice is

$$M_1 = \hat{u}\Gamma, \qquad \hat{u} = \frac{u_1 + u_2}{2},$$

but this is not dictated by any physical principle. What makes it convenient is that the total kinetic energy equation is the same as it was with $M = 0$, that is,

$$\sum_{i=1}^{2} [\partial_t(\tfrac{1}{2}\alpha_i\rho_i u_i^2) + \partial_x(\tfrac{1}{2}u_i\alpha_i\rho_i u_i^2) + u_i\alpha_i\partial_x p] = 0. \tag{3.1.3}$$

We leave this to the reader, but the following relations will help. For any f, let

$$D_i f = \partial_t f + u_i\partial_x f,$$
$$D_i^c f = \partial_t(\alpha_i\rho_i f) + \partial_x(\alpha_i u_i\rho_i f).$$

Then

$$D_i^c f = \alpha_i\rho_i D_i f + f\Gamma_i. \tag{3.1.4}$$

Use this with (3.1.2) and $f = u_i$ to get an expression for $D_i u_i$. Then use it again with $f = \frac{1}{2}u_i^2$ to get (3.1.3).

It follows from (3.1.3) that total energy will be conserved if

$$\begin{gathered}\partial_t(\alpha_i\rho_i e_i) + \partial_x(\alpha_i\rho_i e_i u_i) + p[\partial_t\alpha_i + \partial_x(\alpha_i u_i)] = L_i, \\ L_1 = -L_2 = L\Gamma.\end{gathered} \tag{3.1.5}$$

Then L is the latent heat of vaporization, which like Γ must be given as a function of the other variables.

Without mass transfer, the assumption of entropy conservation for each phase led us to the correct form of the internal energy evolution equation. Now, having the correct energy equation we can find the entropy evolution equation. Several applications of (3.1.4) and the fact that $\alpha_i D_i(\rho_i) = \Gamma_i - \rho_i[\partial_t\alpha_i + \partial_x(\alpha_i u_i)]$ produce

$$\partial_t(\alpha_i\rho_i S_i) + \partial_x(\alpha_i\rho_i u_i S_i) = \left\{S_i - \frac{1}{T_i}\left[e_i + \frac{p}{\rho_i}\right] + \frac{L}{T_i}\right\}\Gamma_i. \tag{3.1.6}$$

and therefore

$$\begin{aligned}D_1^c S_1 + D_2^c S_2 = &\left\{S_1 - S_2 - \frac{1}{T_1}\left[e_1 + \frac{p}{\rho_1}\right] + \frac{1}{T_2}\left[e_2 + \frac{p}{\rho_2}\right]\right\}\Gamma \\ &+ L\left(\frac{1}{T_1} - \frac{1}{T_2}\right)\Gamma.\end{aligned} \tag{3.1.7}$$

Let

$$\Phi = S_1 - S_2 - \frac{1}{T_1}\left[e_1 + \frac{p}{\rho_1}\right] + \frac{1}{T_2}\left[e_2 + \frac{p}{\rho_2}\right].$$

The second law of thermodynamics requires that the right side of (3.1.7) be nonnegative, i.e.,

$$\left[\Phi + L\left(\frac{1}{T_1} - \frac{1}{T_2}\right)\right]\Gamma \geqslant 0. \tag{3.1.8}$$

This is a *constraint* on Γ and L; a simple way to satisfy it would be to set

$$\Gamma = r\left[\Phi + L\left(\frac{1}{T_1} - \frac{1}{T_2}\right)\right].$$

for some positive constant r.

In the special case $T_1 = T_2$, the constraint on Γ agrees with intuitive notions of boiling and condensation. To see this suppose the fields are described by a van der Waals equation of state (see [23]). The latter has the form shown in Fig. 3.1. The line AB is called the Maxwell line and is defined by the condition that the area in the loops above and below the line are equal. Suppose that the curve for $v < v_C$ represents field 2, and that it represents field 1 for $v > v_D$. Since $TdS = de + pvd$, the equal area condition says that it field 2 is in state P_A, v_A, e_A, S_A, T_A, and field 1 in state P_B, etc., with $p_A = p_B = p$, $T_A = T_B = T$, then

$$S_A - S_B - \frac{1}{T}\left[e_A + \frac{p}{\rho_A}\right] + \frac{1}{T}\left[e_B + \frac{p}{\rho_B}\right] = 0.$$

Since all the variables can be expressed as functions of T and p, this defines p as a function $p_{SAT}(T)$. Then a mixture of the fields is in equilibrium—meaning that the entropy of the mixture is greater than the entropy of any other mixture—if

$$T_1 = T_2 = T,$$
$$p_1 = p_2 = p = p_{SAT}(T),$$
$$u_1 = u_2 = u.$$

(This also defines an equilibrium mixture equation of state, which will be discussed in Sect. 4.)

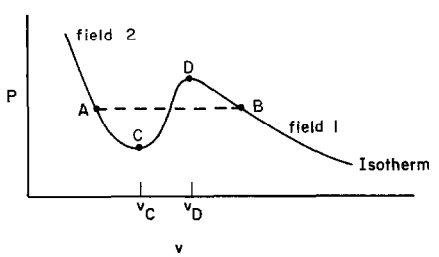

FIG. 3.1. Van der Waals isotherm.

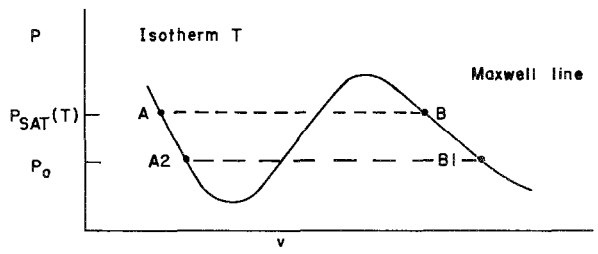

FIG. 3.2. Nonequilibrium pressure.

Now, suppose our two fields are at the same temperature, $T_1 = T_2 = T$, but not in equilibrium. Suppose for $p = p_0$, $\Phi > 0$. If the line $A2B1$ in Fig. 3.2 is at pressure p_0 then the area of the loop above the line $A2B1$ is greater than the area of the loop below $A2B1$. But then $A2B1$ is below AB, that is, $p_0 < p_{SAT}(T)$. But this is when we expect boiling to occur, that is, $\Gamma > 0$. If $\Phi < 0$, then it is easily seen that $p_0 > p_{SAT}$, which leads to condensation, i.e., $\Gamma < 0$.

3.2. *Mutual Forces*

Any force that one field exerts on the other must appear in both the momentum and energy equations. To the right side of (3.1.2) must be added a term F_i, with

$$F_1 = -F_2 = F.$$

Then (3.1.3) becomes

$$\sum_{i=1}^{2} [\partial_t(\tfrac{1}{2}\alpha_i\rho_i u_i^2) + \partial_x(\tfrac{1}{2}u_i\alpha_i\rho_i u_i^2) + u_i\alpha_i\partial_x p] = (u_1 - u_2)F.$$

An important, if not *the* most important force is frictional drag, for which

$$F = \lambda(u_2 - u_1), \qquad \lambda > 0$$

(λ has dimensions density over time). Then

$$(u_1 - u_2)F = -\lambda(u_1 - u_2)^2.$$

Now the L_i in (3.1.5) must have the form

$$L_1 = L\Gamma + \theta\lambda(u_1 - u_2)^2,$$
$$L_2 = -L\Gamma + (1-\theta)\lambda(u_1 - u_2)^2.$$

For the total entropy we can have

$$D_1^c S_1 + D_2^c S_2 = \left[\Phi + L\left(\frac{1}{T_1} - \frac{1}{T_2}\right)\right]\Gamma + \lambda\left(\frac{\theta}{T_1} + \frac{1-\theta}{T_2}\right)(u_1 - u_2)^2,$$

so the frictional drag increases the total entropy (in fact, it does not decrease the entropy of either field). One problem here is that the choice of θ is not at all clear, although it would seem that θ should vary directly with α.

There are other forces that can be important. Among these is the force due to virtual mass. Attempts to model this effect in one dimension are to be found in [2, 24–27]. These references do not agree on the form of virtual mass terms.

3.3. *Surface Tension, Heat Conduction, and Viscosity*

The importance of these effects will of course depend on the particular application. To be completely correct they should be included at the outset in the complete local description of the flow, as in [1]. Here, we shall simply note those terms that need to be added to the basic model.

Surface tension can be accounted for by using, instead of $p_1 = p_2 = p$, the relation $p_1 = p$, $p_2 = p + \sigma\partial^2\alpha/\partial x^2$ (in 1-dimension). With surface tension the basic model becomes well-posed, as shown in [28].

Heat conduction is included by replacing $L\Gamma$ in Subsection 3.1 by $L\Gamma + K(T_2 - T_1)$.

Viscosity of the individual phases is accounted for by adding $\mu_i(\partial^2 v_i/\partial x^2)$ to the right side of the ith momentum equation. One should also consider turbulent mixing, but this lies outside the scope of this paper.

3.4. *Practical Limitations*

In any set of averaged equations details of the interface between the phases are suppressed, by design. However, accurate modeling of interfacial transfer terms requires some knowledge of the interface. For example, the coefficient λ in the friction (Subsect. 3.2) will certainly vary with the area of the interface. One could imagine having an additional differential equation describing the transport of average interfacial area or of additional topological information, as in [29], but the idea has not been sufficiently developed to be generally useful. Current models use experimentally determined correlations for interfacial area as functions of the other dependent variables. These often involve flow-regime maps: the flow topology is assumed known in each region, e.g., bubbly in one region, stratified in another, etc. In each regime the results of experiments with the particular type of flow encountered are used to obtain the necessary correlations. This assumes that in application the flow regime is always fully developed.

The use of flow-regime maps is an example of one compromise among many that must be introduced in order to obtain a working, useful code. These compromises severely limit the achievable accuracy of these codes.

4.0. *Limiting Cases*

The six (in one space dimension) partial differential equations of the basic model are a description of the nonequilibrium flow of two fields. In some applications it

might be known that partial equilibria exist, leading to simpler models. Some of these are presented below.

4.1. *Equal Velocities*

If the friction is very large, the two fields will move with nearly equal velocities. We may then approximate this by supposing that the velocities are identically equal. The two momentum equations must be replaced by the total momentum equation. In order to compute the speed of sound for this system it is convenient to rewrite it in a different form. Let

$$\rho = \alpha\rho_1 + (1-\alpha)\rho_2,$$

$$q = \frac{\alpha\rho_1}{\rho}.$$

Then the differential equations are

$$\partial_t \rho + \partial_x(\rho u) = 0,$$

$$\rho[\partial_t u + u\partial_x u] + \partial_x p = 0,$$

$$\partial_t S_1 + u\partial_x S_1 = \frac{1}{\rho_1 q T_1}\left[L - e_1 - \frac{p}{\rho_1}\right]\Gamma,$$

$$\partial_t S_2 + u\partial_x S_2 = \frac{1}{\rho_2(1-q)\,T_2}\left[e_2 + \frac{p}{\rho_2} - L\right]\Gamma,$$

$$\partial_2 q + u\partial_x q = \frac{\Gamma}{\rho}.$$

This is a hyperbolic system; if each field is compressible then the characteristic speeds are $u + c_e, u - c_e, u, u, u$, where

$$\frac{1}{\rho^2 c_e^2} = \frac{q}{(\rho_1 c_1)^2} + \frac{1-q}{(\rho_2 c_2)^2}. \tag{4.1.1}$$

This has an interesting consequence. Suppose field 1 is air, and suppose field 2 is water. Then

$$\frac{dc_e^2}{dq} < 0, \qquad q = 0,$$

$$= 0, \qquad q \cong \rho_l/\rho_2,$$

$$> 0, \qquad q = 1,$$

so $c_e^2(q)$ has the form shown in Fig. 4.1. For $q \cong \rho_1/\rho_2$, the speed of sound of the mixture is less than the sound speed of both fields.

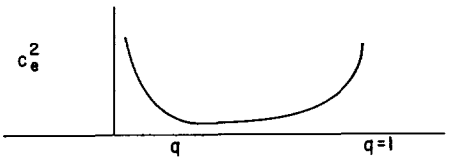

FIG. 4.1. Mixture sound speed.

If we consider air to be a gamma-law gas, then for an air–water mixture

$$c_e \cong \sqrt{\gamma p/\alpha(1-\alpha)\rho_2}.$$

Since $\rho_2 \cong 1000\,\rho_1$, if $\alpha = \frac{1}{2}$,

$$c_e \cong \tfrac{1}{16} c_{\text{air}}.$$

4.2. *Asymptotics and Drift Flux*

Consider a system of partial differential equations

$$L(u) = \lambda B u,$$

where L is a nonlinear differential operator and B is a matrix of rank $K < n$ (in the examples the rank of B is 1). Try

$$u = \sum_{i=0}^{\infty} u^i \lambda^{-i}.$$

Then

$$L\left(u^0 + \frac{1}{\lambda}\sum_{i=1}^{\infty} u^i \lambda^{-i+1}\right) = \sum_{i=0}^{\infty} B u^i \lambda^{i+1}.$$

Thus

$$Bu^0 = 0$$

and

$$L(u^0) = Bu^1.$$

Let P be a projection onto the nullspace of B. The equations

$$Bu^0 = 0, \qquad PL(u^0) = 0$$

determine the lowest order approximation u^0. The next order satisfies

$$L'(u^0)\, y^1 = Bu^2.$$

Then the equations

$$L(u_0) = Bu^1, \qquad PL'(u^0)\, u^1 = 0$$

have to determine u^1. It is more convenient to combine the two approximations in one nonlinear problem. Let

$$w = u^0 + (1/\lambda)\, u^1,$$

then

$$BW = \frac{1}{\lambda} Bu^1 = \frac{1}{\lambda} L(u^0) = O\left(\frac{1}{\lambda}\right).$$

Furthermore

$$PW = \frac{1}{\lambda} L\left(u^0 + \frac{1}{\lambda} Pu^1\right) + O\left(\frac{1}{\lambda}\right)^2 = \frac{1}{\lambda} L(PW) + O\left(\frac{1}{\lambda}\right)^2$$

and

$$0 = P\left[L(u^0) + \frac{1}{\lambda} L^1(u^0)\, u^1\right] = PL(W) + O\left(\frac{1}{\lambda}\right)^2.$$

Therefore, up to terms of order $O(1/\lambda)^2$ the original system can be replaced by

$$PL(W) = 0, \qquad BW = (1/\lambda)\, L(PW).$$

EXAMPLE. Consider the momentum equations in the two-fluid model:

$$\frac{\partial}{\partial t} \rho_1 \alpha_1 v_1 + \frac{\partial}{\partial x} \rho_1 \alpha_1 (v_1)^2 + \alpha_1 \frac{\partial p}{\partial x} = \lambda (v_2 - v_1),$$

$$\frac{\partial}{\partial t} \rho_2 \alpha_2 v_2 + \frac{\partial}{\partial x} \rho_2 \alpha_2 (v_2)^2 + \alpha_2 \frac{\partial p}{\partial x} = -\lambda (v_2 - v_1).$$

Here,

$$B\binom{r}{s} = \binom{s-r}{r-s}.$$

Take

$$P\binom{r}{s} = \binom{r+s}{r+s},$$

then

$$PB = 0,$$

and

$$PL(W) = \frac{\partial}{\partial t} (\rho_1 \alpha_1 v_1 + \rho_2 \alpha_2 v_2) + \frac{\partial}{\partial x} (\rho_1 \alpha_1 (v_1)^2 + \rho_2 \alpha_2 (v_2)^2) + \frac{\partial p}{\partial x} = 0.$$

Using the continuity equations, $L(PW) = \lambda BW$ consists of the equations

$$\rho_1 \alpha_1 \left(\frac{\partial}{\partial t} (v_1 + v_2) + (v_1 + v_2) \frac{\partial}{\partial x} (v_1 + v_2)\right) + \alpha_1 p_x = \lambda (v_2 - v_1),$$

$$\rho_2 \alpha_2 \left(\frac{\partial}{\partial t} (v_1 + v_2) + (v_1 + v_2) \frac{\partial}{\partial x} (v_1 + v_2)\right) + \alpha_2 p_x = -\lambda (v_2 - v_1),$$

or

$$v_2 = v_1 + \frac{\alpha_1\alpha_2(\rho_2 - \rho_1)}{\lambda(\alpha_1\rho_1 + \alpha_2\rho_2)}\, p_x. \tag{4.2.1}$$

This is the well-known drift flux approximation [1]. It is the analogue of D'Arcy's law for flow in porous media.

The full drift flux model has five partial differential equations; the two momentum equations of the basic model can be replaced by the single equation

$$\partial_t(\rho_1\alpha_1 v_1 + \rho_2\alpha_2 v_2) + \partial_x(\rho_1\alpha_1 v_1^2 + \rho_2\alpha_2 v_2^2) + \partial_x p = 0,$$

using (4.2.1) to eliminate v_2. Another form of this is as follows: Let

$$\bar{v} = \frac{\alpha_1\rho_1 v_1 + \rho_2\alpha_2 v_2}{\alpha\rho + \alpha\rho},$$

$$\bar{\rho} = \alpha_1\rho_1 + \alpha_2\rho_2,$$

then

$$\bar{\rho}(\partial_t\bar{v} + \bar{v}\partial_x\bar{v}) + \partial_x\left[\frac{1}{p}\,\alpha_1\alpha_1\rho_2\rho_2(v_2 - v_1)^2\right] + \partial_x p = 0,$$

or

$$\bar{\rho}(\partial_t\bar{v} + \bar{v}\partial_x\bar{v}) + \partial_x\left[\frac{(\alpha_1\alpha_2)^3}{\lambda^2(\bar{\rho})^3}\,(\rho_1\rho_2)^2\,(\rho_2 - \rho_1)^2\,(\partial_x p)^2\right] + \partial_x p = 0.$$

4.3. *Homogeneous Equilibrium*

In this model, we assume that everything is in equilibrium at the outset. This means that $v_1 = v_2 = v$, $T_1 = T_2 = T$, and

$$S_1 - \frac{1}{T}\left[e_1 + \frac{p}{\rho_1}\right] = S_2 - \frac{1}{T}\left[e_2 + \frac{p}{\rho_2}\right]. \tag{4.3.1}$$

The differential equations are the single-phase gas-dynamic equations, for which we have to provide an equation of state, say $p = p(\rho, S)$, where ρ and S are the mean density and entropy, respectively. This is done as follows: We have

$$\frac{1}{\rho} = \frac{q}{\rho_1} + \frac{1-q}{\rho_2} \tag{4.3.2}$$

and

$$S = qS_1 + (1-q)\,S_2. \tag{4.3.3}$$

If we take p and T to be the independent thermodynamic variables for the individual phases, then Eq. (4.3.1) defines T as a function of p, the so-called saturation curve. Then Eqs. (4.3.2) and (4.3.3) are solved for p and q as functions of ρ and S.

The sound speed is $\partial p(\rho, S)/\partial \rho = c_H^2$. This is obtained by differentiating Eqs. (4.3.2), (4.3.3) with the respect to ρ. Noting that, from Eq. (4.3.1), $(1/\rho_1 - 1/\rho_2)/(S_1 - S_2) = dT/dp$, we get

$$\frac{1}{c_H^2 \rho^2} = q\left(\frac{1}{\rho_1^2}\frac{d\rho_1}{dp} + \frac{dS_1}{dp}\frac{dT}{dp}\right) + (1-q)\left(\frac{1}{\rho_2^2}\frac{d\rho_2}{dp} + \frac{dS_2}{dp}\frac{dT}{dp}\right).$$

After some tedious manipulation with Maxwell's relation, we find

$$\frac{1}{\rho^2 c_H^2} = \frac{q}{\rho_1^2 c_1^2} + \frac{1-q}{\rho_2^2 c_2^2} + q\left(\frac{\partial S_1}{\partial T}\right)_P \left[\left(\frac{\partial S_1}{\partial v}\right)_P \left(\frac{dT}{dP}\right) - 1\right]^2$$
$$+ (1-q)\left(\frac{\partial S_2}{\partial T}\right)_P \left[\left(\frac{\partial S_2}{\partial v}\right)_P \frac{dT}{dP} - 1\right]^2.$$

Thus $c_H^2 \leqslant c_e^2$ if $(\partial S_i/\partial T)_P \geqslant 0$. This is an example of the general situation that the equilibrium sound speed is not greater than the frozen sound speed [6]. Computations in [30] show that this speed is as low as 10 ft/s for low values of q.

II. Methods

5.0. *Theoretical Considerations for Numerical Methods*

We now turn from the intricacies of modelling 2-phase flow, and consider the question of solving the differential equations for problems of practical interest. Of course, numerical approximate methods are the only practical choice. It may seem rash to solve a set of equations which are not known to be correct in detail. The effort is justified in many cases because numerical solutions yield information of practical value even admitting some uncertainty. More basically, numerical solutions help evaluate the uncertainty and improve the model. To achieve this, one must understand the numerical methods and their limitations. The numerical cart will not draw the physical horse, but both are needed.

As in Part I, we consider flows with two continuous fields of velocity. To keep the discussion of methods as general as possible, we mention only the barest features of typical interfacial terms; varying the details of interphase exchange terms perturbs numerical schemes in a secondary way, and the first task is to master the left-hand side of the equations. Experience confirms this, since interphase exchanges are usually local in nature. The presence of exchange terms influences the basic design of numerical methods, but their particular form seldom does. Even the inclusion of virtual mass terms, which contain derivatives of the unknowns, usually amounts to variations on a theme, because the derivatives have the same form as the fluid

convection terms already present. If we concentrate on the left-hand side here, it is not because we are uncritically following the emphasis of Part I; on the contrary, experience with numerical schemes tends to confirm the wisdom of that emphasis.

The equations whose numerical solution we will consider are

$$\begin{aligned} \partial_t \alpha_i \rho_i + \nabla \cdot \alpha_i \rho_i \mathbf{v}_i &= \Gamma_i \\ \partial_t \alpha_i \rho_i \mathbf{v}_i + \nabla \cdot \alpha_i \rho_i \mathbf{v}_i \mathbf{v}_i + \alpha_i \nabla p &= M_i - F_i \\ \partial \alpha_i \rho_i e_i + \nabla \cdot \alpha_i \rho_i e_i \mathbf{v}_i + p[\partial_t \alpha_i + \nabla \cdot \alpha_i \mathbf{v}_i] &= L_i. \end{aligned} \tag{5.0.1}$$

With emphasis on the terms on the left side, we assume for simplicity that the exchange term on the right (see Chap. 3) are algebraic functions of the principal unknowns, which we take to be α (one of the two α_i), p, the internal energies e_i, and velocities $\mathbf{v}_i$.

The major change in viewpoint from Part I is that we will give special consideration to multidimensional problems. To discuss only solution methods for 1-dimensional problems would be seriously misleading. As is usual in solving partial differential equations numerically, the increased effort required to pass from one space dimension to two or three may require wholly different methods. As the difficulties increase, so do the benefits of clearly understanding the relation between problem physics and numerical methods. We shall see examples of this below.

The equations for 2-phase flow above can be applied to a broad range of physical flow configurations. Some features of the solutions, for example, shock waves, may be significant in some applications and not in others. It is a vain hope that one method of solution will be best for all applications. Therefore we shall discuss the methods in several existing codes, indicating the physical conditions for which they are most appropriate.

5.1. *Scales*

To help sort out the various numerical methods it is convenient to identify three classes of physical phenomena contained within the basic 2-phase flow equations. These are interphase exchanges, fluid convection, and sonic propagation. Each has a characteristic time scale. The exchange terms often take the form: rate expression $\times$ deviation from equilibrium (mechanical of thermal). In this case the characteristic time is the inverse of the rate; for example, if the momentum exchange F_i included a drag force,

$$\partial_t \mathbf{v}_i + \cdots = \frac{k}{\alpha_i \rho_i} (\mathbf{v}_j - \mathbf{v}_i) + \cdots, \tag{5.1.1}$$

characteristic time $= \alpha_i \rho_i / k$. For convection, the characteristic time is the time for either phase to move in any direction a distance equal to the grid spacing in that direction. For sonic propagation, it is the time for a small pressure disturbance to travel one grid step.

Efficient difference schemes are those in which computational effort concentrates on features of the solution which have practical significance. For example, in analyzing the sudden accidental depressurization of a nuclear reactor, rarefaction waves need to be followed through the core for a very short time to determine mechanical stresses. After the pressure waves die down, there is presumably no need for a numerical method which accurately resolves them. Thermal disequilibrium between phases is important near the break for a substantial length of time. Mechanical disequilibrium (i.e., flow separation) is not important anywhere in the reactor vessel until later times. The effects of convection can be ignored during the first instants.

In a typical 2-phase flow problem the characteristic times might be of the order of 10^{-5} s for interphase exchanges, 10^{-3} s for pressure propagation, and 10^{-1} s for convection. If these time scales applied to the early moments of the depressurization problem, where tracking pressure waves is important, we would apply forward (i.e., explicit) differences to pressure propagation terms and compute on a time scale of 10^{-3} s. Even though the details of convection are unimportant, there is no advantage to implicit (i.e., backward) convection differencing in this case. Interphase exchanges would probably be differenced implicitly if (as is usually the case) the resulting coupling of unknowns can be solved with modest computational effort. This would yield solutions with roughly correct disequilibrium (e.g., $\mathbf{v}_1 - \mathbf{v}_2$) if the disequilibrium changes slowly. If rapid fluctuations in disequilibrium must be resolved accurately, a fully explicit solution would be needed, which could be costly due to the exceedingly small time step size imposed.

The idea that Eqs. (5.0.1) represent several distinct phenomena is so useful that we will also write the two-fluid equations simply as

$$w_t + Ew + Sw + Cw = G, \tag{5.1.2}$$

where w is a vector of unknown flow variables and E, S, C are operators describing the effects of interfacial exchanges, sonic propagation, and convection, respectively. This equation should be taken with a grain of salt, as the true equations are nonlinear; still the decomposition is meaningful and deserves a shorthand notation.

For a closer description, let $w = (r, \mathbf{q})$, where r stands for the state variables p, α, e_1, e_2, and $\mathbf{q}$ stands for velocity vectors $\mathbf{v}_1$ and $\mathbf{v}_2$; the mass and energy equations are

$$r_t + cr + s\mathbf{q} + er = g, \tag{5.1.3}$$

and the equations of motion are described by

$$\mathbf{q}_t + \mathbf{cq} + \mathbf{s}r + \mathbf{eq} = \mathbf{g},$$

where

$$C = \begin{pmatrix} c & 0 \\ 0 & \mathbf{c} \end{pmatrix}, \qquad E = \begin{pmatrix} e & 0 \\ 0 & \mathbf{e} \end{pmatrix}, \qquad S = \begin{pmatrix} 0 & s \\ \mathbf{s} & 0 \end{pmatrix}.$$

5.2. *Stability*

Since the single-pressure equations of the two-fluid model form an ill-posed initial value problem, the reader may well ask why standard finite difference schemes are usable at all. Any consistent scheme for these equations is in mathematical terms unconditionally unstable, i.e., for any constant ratio $\Delta t/\Delta x$, geometrically growing instabilities will always appear if Δx is made sufficiently small. This contradicts our expectation that for appropriate flow conditions the averaging process leading to equations (5.0.1) can smooth out small-scale fluctuations altogether so that the equations have a steady solution. This in turn corresponds to our perception of experimental data as describing a steady state if the data show only high frequency noisy fluctuation about an unchanging average value. In practice, numerical schemes have been used to obtain reasonable results for a variety of problems. For example, steady state solutions are usually obtained when expected, with no evidence of instability after thousands of computed time steps. We wish to understand better why this is so.

For practical computation, it would be unusual to pose a 2-phase flow problem for bubbly flow, define averaged equations with an averaging volume large enough to filter out the effects of individual bubbles, and then solve the equations on a computational grid with cells much smaller than bubble size. Mathematical ill-posedness is an instability in the limit of very fine scale, a scale that is neglected when averaged equations are used. If we insist on well-posed initial value problems, this does not necessarily change things on the scale which passes through the averaging filter.

If reasonable numerical results are obtained from the ill-posed single pressure model, a numerical filter must be present. This is the role played by dissipative terms. An analysis of the stability of some popular difference equations has been carried out [35]. The results, in brief, were as follows. First, it was assumed (somewhat arbitrarily) that a necessary condition for well-behaved numerical solutions is that von Neumann local linear stability analysis reveal no geometrically growing modes, that is, no eigenvalue of the amplification matrix shall have magnitude greater than unity. This will result if three competing factors are in balance, namely, the ill-posedness of the equations, the physical damping due to interphase exchange terms, and the numerical damping due to donor cell differencing. The ill-posedness will produce instabilities if not balanced by exchange terms (which damp low frequencies) and by numerical diffusion (at high frequencies). Numerical diffusion suppresses instabilities on the scale of a few mesh cells. The extent of damping due to exchange terms can be judged from their built-in length scale. For a typical bubbly flow drag term, analysis showed this to be comparable to the bubble radius. That is, interfacial drag damps wavelengths larger than bubble size. Geometrically growing modes are then absent if the damped wavelength ranges overlap, that is, if mesh size is coarser than bubble size. This gives a physically comprehensible necessary condition for numerical solutions of (5.0.1) to be well behaved.

Still there are substantial questions about the ill-posed model. We do not have an

option of using very fine grids to generate an exact solution. Even to estimate the size of errors due to numerical approximations may be difficult. For a given problem we expect there will be a mesh size yielding minimum error; but as the mesh is further refined, the symptoms of ill-posedness may be hard to identify in a complicated problem.

A most important aspect of the stability question, both in modelling and in numerical methods, is this: Will a model describe the real physical instabilities which are important, without introducing uninteresting or spurious oscillations? To appreciate some of the unanswered questions about Eqs. (5.0.1) and ill-posedness, let us look at a real flow experiment [36]. Consider a half-inch thick box one foot wide and three feet high; an air-water mixture is injected in the middle of the bottom end and flows out either side near the far (top) end. The 2-phase flow in the box is bubbly and highly agitated. By recording averages over several minutes, void fraction measurements are taken at a number of locations. These space–time averaged values persist and are reproducible.

Such a flow can be modelled using a semi-implicit finite difference method for Eqs. (5.0.1). Using roughly 100 mesh cells and 2 ms time steps, numerical solutions typically show fluctuations of the mass flow rate at the outlet (for steady inflow). The rate of oscillation is on the order of once per second. Computed solutions show no oscillation when the phase velocities are equal, but this would require unphysically large interfacial drag. Fluctuating numerical solutions can be averaged over time to give void fractions in fair agreement with the long-time averages recorded from the experiments. Figure 5.1 shows some of the computed oscillations in outlet flow rate for different interfacial drag forces (determined by a parameter analogous to bubble radius).

Among the questions raised are these: Does the real flow oscillate on the same time scale as the calculations? Are the oscillations periodic or aperiodic, or both? How sensitive are the calculated oscillations to mesh size, numerical convergence, and changes in modelling? How do power spectra from computations compare with experimental spectra of, say, acoustic noise? Are these transition scenarios observable by varying inlet flow rate in the experiment? If the oscillations are an artifact of the model, what specific changes in the differential equations are needed? Questions such as these are likely to be more productive than dry theory.

6.0. *Eulerian Finite Difference Methods*

By far, the most common approach to solving Eqs. (5.0.1) numerically is a finite difference scheme on an Eulerian grid. In view of the complexity of the basic equations, not to mention the flow environment in a typical application, just to assemble a complete repertory of efficient low-order finite difference methods is a nontrivial goal. The essential issues are the choice of difference grid, the representation of differences on the grid (particularly implicit versus explicit), and the method of solving the difference equations.

6.1. *The Grid*

Efficient methods are most easily formulated on the staggered mesh, now almost universal in two fluid codes. As illustrated in Fig. 6.1 (for the case of the two space dimensions), the computational region is composed of rectangles, with integer grid points located in the center of each cell. Fluid state properties, such as density, internal energy, temperature, pressure, and void fraction have their principal point at the centers; values at cell faces are determined by interpolation. Velocity components have principal points at the midpoints of cell faces normal to them; u is the x component, v is the y component. The generalization to three dimensions is clear. To minimize subscripts, we omit either index if it corresponds to the principal point.

The staggered grid is particularly convenient for difference schemes where sonic propagation is treated implicitly. As we shall see, the equations for the unknowns then have a simple structure when the staggered grid is used.

6.2. *Semi-implicit Schemes*

A principle distinction among finite difference methods for 2-phase flow is the extent to which backward time differences are used. In differencing equations describing several phenomena, one need not hold to uniform backward or forward differences, but can choose term by term based on physical phenomena. One may treat say, interphase exchange implicitly while differencing convective terms explicitly if this gives a more efficient method. The main criteria are the characteristic times and the physical phenomena of interest, as discussed above.

In compressible 2-phase flow problems not requiring resolution of shock or pressure waves in great spatial detail, it may be advantageous to apply backward differences to the terms describing sonic propagation. Since characteristic times for exchanges are usually as restrictive as sonic propagation times, exchange terms should be treated implicitly as well. For the moment we will examine methods implicit to this extent but explicit in the remaining terms describing fluid convection. Such methods are appropriate for a large number of problems, and were pioneered by Liles and Reed [37]. In the shorthand of Eq. (5.1.2), these methods solve

$$(\Delta t^{-1} + E + S)\, w^{n+1} = (\Delta t^{-1} - C)\, w^n + G.$$

To allay any fears that implicit differencing may fail for equations with complex characteristics, let us consider for a moment the model problem

$$\phi_t + (1 + \varepsilon i)\, \phi_x + K\phi = 0. \tag{6.2.1}$$

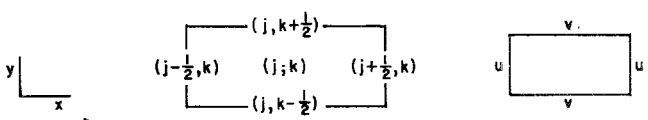

FIG. 6.1. A cell in the staggered mesh with grid point indices.

Recalling the role of interfacial drag mentioned in Subsection 5.2, we include the damping term $K\phi$. An implicit scheme for this equation is

$$(\phi_j^n - \phi_j^{n-1})/\Delta t + (1 + \varepsilon i)(\phi_j^n - \phi_{j-1}^n)/\Delta x + K\phi_j^n = 0. \tag{6.2.2}$$

The amplification factor λ for a wave having period $m\Delta x$ is given by

$$\lambda^{-1} = 1 + (\Delta t/\Delta x)\{K\Delta x + (1 + \varepsilon i)[1 - \exp(-i\pi/m)]\}. \tag{6.2.3}$$

For $K = \varepsilon = 0$, the locus of λ^{-1} is on a circle outside the unit circle in the complex plane, and tangent to the unit circle at the point 1 on the real axis. (See Fig. 6.2,

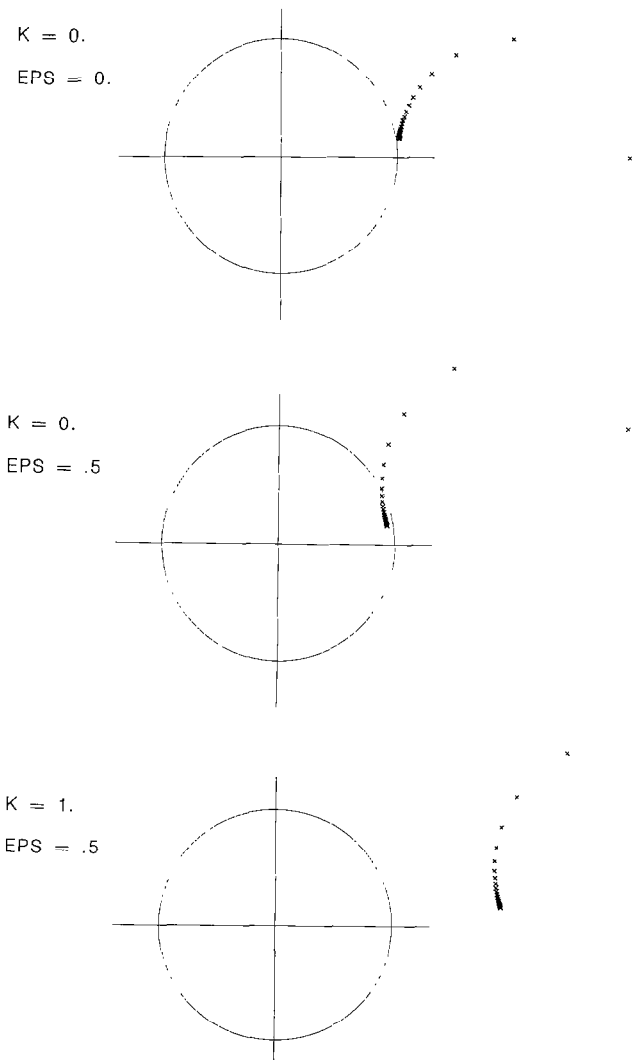

FIG. 6.2. Locus of Eq. (6.2.3) relative to the unit circle.

where $\Delta x = \Delta t = 1$ is assumed, and $m = 1,..., 20.$) Allowing $\varepsilon > 0$ tilts this locus about the point of tangency, throwing part of the locus inside the unit circle, which indicates instability. But for any $\varepsilon > 0$, there is a value $K\Delta x > 0$ above which the locus will be shifted outside the unit circle. That is, if Δx is not too small relative to ε and K, (6.2.3) suggests that the difference scheme (6.2.2) is stable for all Δt. Note also that for small $k\Delta x$ it is the *long* wavelengths which grow.

The expected analogous result for Eqs. (5.0.1) in semi-implicit differences is established in [35].

Now let us describe the semi-implicit difference equations in two dimensions; the extension to three dimensions is straightforward. Keeping in mind that sonic propagation and phase change are treated implicitly, convection explicitly, the difference equations for mass conservation are

$$\alpha_i^{n+1}\rho_i^{n+1} - \alpha_i^n\rho_i^n + \frac{\Delta t}{\Delta x}\left[\alpha_i^n\rho_i^n u_i^{n+1}\right]_{j-1/2}^{j+1/2} - \frac{\Delta t}{\Delta y}\left[\alpha_i^n\rho_i^n v_i^{n+1}\right]_{k-1/2}^{k+1/2} = \Gamma^{n+1}\Delta t, \tag{6.2.4}$$

where $n+1$ and n are new and old time levels, respectively; the brackets indicate mass flux differences between the cell faces at $j+1/2$ and $j-1/2$, for example. Remember that i indicates the phase; j's and k's may be suppressed according to our principal point convention. Clearly it is convenient to identify the mass flux across cell fact $j+1/2$ with $(j+1/2, k)$, the principal point of u_i; likewise for v_i and cell face $k+1/2$. The locations of $\alpha_i\rho_i$ in the mass flux differences, which are ambiguous in the above difference formula, are determined by donor cell rules. It has been found by experience that central differences result in numerical instability for 2-phase flow, even though this is not necessarily true for single-phase flow.

The mass flux differences have $\alpha_i\rho_i$ at time n, but u_i, v_i at time $n+1$. The reasoning behind this is clarified by considering

$$\partial_x(\alpha_i\rho_i u_i) = \partial_x(\alpha_i\rho_i)\, u_i + \alpha_i\rho_i\partial_x(u_i).$$

The derivative of $\alpha_i\rho_i$ would make no contribution if $u_i = 0$, which is the case of no convection; so the $\alpha_i\rho_i$ difference describes the effect of convection and is differenced explicitly. The u_i and v_i differences propagate pressure waves, as can be seen by applying ∂_t to

$$\partial_t p + \rho\partial_x u = \cdots,$$

and ∂_x to

$$\rho\partial_t u + \partial_x p = \cdots.$$

Subtracting the two results and recalling that $\partial\rho/\partial p = c^{-2}$, we obtain a wave equation for p,

$$c^{-2}\partial_{tt} p - \partial_{xx} p = \cdots.$$

To appreciate the convenience of the staggered grid, notice that on the left side of the mass difference equation (6.2.4), all new time unknowns appear at their principle points because of the staggered grid. The same is true on the right side; Γ is required at the cell center where the most influential variables α, p, e_i have their principle point. (If cell centered new time velocities appear in Γ, they can be written as averages of cell face values, but the dependence of Γ on velocities is usually not so strong as to require new time values for stability.)

The above argument for obtaining a wave equation also cues the selection of backward differenced terms in the momentum equations

$$(\alpha_i\rho_i)_{j+1/2}\,(u_i^{n+1}-u_i^n)+\text{convection terms}+\frac{\Delta t}{\Delta x}\,(\alpha_i)_{j+1/2}\,[p^{n+1}]_j^{j+1}$$
$$=\Delta t(M_i^x-F_i^x)_{j+1/2,k}^{n+1} \tag{6.2.5}$$

and similarly for v_i. We have changed the form of the momentum equation using Eq. (3.1.4) which alters M_i. The convection terms are all explicit, involving donor cell rules. On the left side we again see that the $n+1$ time unknowns appear at their principal points. The right-hand side will be discussed presently.

Finally, the energy equations can be differenced in a manner entirely analogous to the mass equations. Notice that the difference scheme would strictly conserve mass and energy if the difference equations were solved exactly; this is important for flow in a closed system.

The resulting set of difference equations (with the equations of state substituted in) gives eight equations for the eight unknowns $\alpha^{n+1}, p^{n+1}, e_i^{n+1}, u_i^{n+1}, v_i^{n+1}$. The nonlinearities in these equations are relaively mild due to the explicit differencing of convection. The main difficulty in solving these equations comes from the spatial coupling of each node to its neighbors and hence inductively to all other nodes. The larger the time step size, the stronger is this spatial coupling. The equations are most efficiently solved by observing that, under very reasonable assumptions, the spatial coupling can be expressed solely in terms of the pressures.

Such a simplification can be achieved in the same way the wave equation for p was obtained above; the mass and momentum equations were combined to eliminate velocities. The condition for doing this with the 2-phase difference equations is that each momentum equation involve only the velocities at one cell face and the neighboring pressure. This in turn limits the $n+1$ level unknowns which may appear in M_i^x to u_i^{n+1} and p^{n+1}, with all other variables at time n. In practice this is usually adequate to insure a stable difference scheme; a common example is the interfacial drag expression, a function primarily of $\mathbf{v}_1-\mathbf{v}_2$.

If this restriction is appropriate, then the x-momentum equations may be combined to give expressions for each u_i separately in terms of the neighboring pressures. Similarly, the y-momentum equations combine to give expressions for the v_i. Substituting the expressions for u_i at $j\pm\frac{1}{2}$ and for v_i at $k\pm\frac{1}{2}$ into the mass and energy equations eliminates all velocities, leaving in each cell four equations for

α, p, e_i at the cell center, and the surrounding pressures. By combining these in each cell, α and the e_i can be eliminated, leaving a relation among the five pressures. In short, one finds the solution of

$$(\Delta t^{-1} + e)\, r^{n+1} + s\mathbf{q}^{n+1} = (\Delta t^{-1} - c)\, r^n + g$$
$$(\Delta t^{-1} + \mathbf{e})\, \mathbf{q}^{n+1} + \mathbf{s} r^{n+1} = (\Delta t^{-1} - \mathbf{e})\, \mathbf{q}^n + \mathbf{g}$$

by inverting $(\Delta t^{-1} + e)$, $(\Delta t^{-1} + \mathbf{e})$, and substituting the second equation in the first to obtain

$$[1 - (\Delta t^{-1} + e)^{-1} s(\Delta t^{-1} + \mathbf{e})\, \mathbf{s}]\, r^{n+1} = \cdots.$$

The easiest way to compute this reduction is first to linearize the difference equations about some guessed solution. The reduction then proceeds by diagonalizing 2×2 and 4×4 matrices for each mesh cell. This could be done by Gaussian elimination, but an absent phase could require pivoting, which can be avoided by using 2×2 matrix inversions. The final pressure equation is a 5-point difference equation which is elliptic. This is natural, since to solve an implicitly differenced wave equation also requires solving an elliptic problem at each time step. In fact, the pressure equation obtained from the 2-phase difference equations is of the form

$$\nabla^2 p + (c\Delta t)^{-2} p = \cdots, \tag{6.2.6}$$

where c is a real quantity identifiable as a sound speed. It is the speed of pressure pulse propagation in the 2-phase mixture taking into account the effects of interphase exchange processes. For example, in the case where only drag-type momentum exchange occurs, one can algebraically perform the reduction to (6.2.6) and identify [39]

$$c^2 = \left\{ \frac{\alpha_1 + k_2}{\rho_1(1 + k_1 + k_2)} + \frac{\alpha_2 + k_1}{\rho_2(1 + k_1 + k_2)} \right\} \Big/ \left(\frac{\alpha_1}{\rho_1 c_1^2} + \frac{\alpha_2}{\rho_2 c_2^2} \right),$$

where k_1 and k_2 are ratios of Δt to the characteristic times for velocity relaxation (cf. Eqs. (5.1.1)). In the limit of no momentum exchange, this approaches the sound speed suggested by the two (real) sonic characteristics of Eqs. (5.0.1). On the other hand, for large k_1, k_2, that is, $k = \alpha_1 \rho_1 k_1 = \alpha_1 \rho_2 k_2 \to \infty$, the expression above tends to the sound speed of the equal velocity model, cf. Eq. (4.1.1). One could similarly work through the reduction for a simple phase change rate expression, and show that it too influences (6.2.6).

The reduction to an elliptic pressure problem is doubly advantageous. The number of unknowns is sharply reduced. And the reduced problem is a familiar one for which a number of powerful methods are available.

Once the pressures are obtained, and the other unknowns determined from them, it may be necessary to linearize the difference equations about these new values of α^{n+1}, p^{n+1}, etc., and reduce again to solve a pressure problem. The resulting Newton iteration usually converges in a very few tries.

The method just described was originally devised for the nuclear reactor safety analysis code TRAC [8]. If its birth certificate is Liles and Reed [37], a fuller biography appears in [39]. The method has since been adopted by several other codes because of its efficiency and robustness. The time step size must be smaller than the characteristic time for convection, but if that limitation is acceptable and the problem admits no simplifying assumptions (such as in dilute gas-particle flows), it is the method of choice. Note that the limit on time step size means there is no direct way of computing a steady flow; a transient calculation must be run with constant forcing terms until the flow becomes steady. In some cases this is very time consuming.

There are two further difficulties with the semi-implicit method just described. One is the numerical diffusion introduced by donor cell differencing; for an understanding of this phenomenon, see [64]. This has the effect of smearing step pulses, either in void or pressure, which may enter the calculation. As seen in the conceptually simple example of a shock hitting a fluidized bed from above, there are open questions about physical dispersion which are just as important as the numerical questions. Since the sonic characteristics of the basic model *are* real, one expects the numerical difficulties to be surmountable for shocks, although for void fronts the ill-posedness might complicate matters.

The second difficulty with the semi-implicit technique is water packing. This is a phenomenon described in [61] whereby artificial pressure spikes appear at a mesh cell just as it fills with a nearly incompressible phase. In practice such spikes are suppressed by an ad hoc procedure setting the compressibility artificially to zero when a cell nears the filling point. In some situations this could, for example, destroy a coincident physical pressure pulse; but usually where pressure waves are important an explicit scheme will be used. Another palliative could be the use of fully implicit differencing.

There is an alternate procedure for solving the same set of semi-implicit difference equations, embodied in the computer code K-FIX [40]. This procedure does not employ the reduction to a pressure problem, but instead performs repeated Gauss–Seidel sweeps over the mesh cells. In each sweep as each cell is visited, all eight principal unknowns are recomputed. This is accomplished in the following way. For a typical cell, suppose cells to the left and below have already been visited. Assuming the pressure in the current cell equals its value from the previous sweep, the velocities across the bottom and left faces can be updated by solving two pairs of momentum equations. Using these newly found velocities on two sides, and taking prior sweep values for the right and upper face velocities, one then has four mass and energy equations for the four unknowns void fraction, pressure, and internal energies of this cell. Solving these gives new values, including a new pressure used in the next step to update velocities between this cell and the next, and so on.

A little reflection shows that this procedure gives essentially the same results as would be obtained by applying Gauss–Seidel iteration to the pressure problem as derived previously. An immediate consequence is that Gauss–Seidel sweeps with either method converge more slowly as $c\Delta t/\Delta x$ increases. Since the point of semi-implicit differencing is to permit $\Delta t \gg \Delta x/c$, slow convergence would be expected with

either solution procedure. In this case the pressure reduction method of solution shows its double advantage: the difficult spatial coupling problem is simplified (one unknown per cell instead of eight or ten), and more powerful techniques can be applied (the problem is elliptic). Of course, certain acceleration techniques can be adapted to the 8-unknown sweep method (overrelaxation and multigrid [41] are examples), but the same improvements are more straightforward and more efficient with the reduced pressure problem.

Another variant of semi-implicit difference solution deserves mention, although it is currently used only for problems involving more than two phases and material components. The SIMMER code [42] for fast reactor accident analysis models three phases of half a dozen material components. In this case the reduction to a pressure problem would involve costly inversions of large matrices in each cell. To speed the computation and save storage, the phase change and sonic propagation terms, although both differenced implicitly, are solved in SIMMER in a way which is not completely coupled. Essentially, the interphase mass and energy exchanges are solved in a first fractional step which treats each cell isolated from the others; that is, the exchanges are coupled to one another within each cell, but pressure propagation to neighbor cells is suppressed. Then in a second fractional step, the interphase exchange *rates* are fixed at the values determined by the first fractional step, and a pressure propagation problem is solved.

This is a type of fractional step method [43] in which the physical phenomena treated in each step are allowed only 1-way coupling, from each step to the succeeding one. At no point are the two sets a phenomena solved with 2-way coupling, so that each can influence the other simultaneously. It is always possible to imagine a situation in which a 1-way coupled fractional step method would fail to be accurate. In the case of the SIMMER approach, consider a liquid–vapor mixture in each of two adjoining cells, such that cell A is experiencing evaporation while cell B has no phase change. Suppose $c\Delta t \gg \Delta x$, so the pressures in each cell are approximately equal at time n and at $n+1$. We assume constant liquid density, saturation vapor density, and liquid phase 2 much denser than vapor phase 1; then the effect of phase change on total void fraction $\alpha = \alpha_1$ is negligible compared to the effect on vapor density, and the semi-implicit method essentially solves

$$(\alpha_A + \alpha_B)(\rho_1^{n+1} - \rho_1^n) \simeq \Gamma_A \Delta t,$$

where Γ_A is the phase change rate in cell A. Now suppose Γ_A is proportional to the departure of cell A conditions from saturation values corresponding to p^{n+1}, and that $\rho_1^{n+1} - \rho_1^n$ is proportional to $p^{n+1} - p^n$; then the phase change rate is limited by pressure buildup. If Γ_A is large, the resulting compression increases p^{n+1} which in turn cuts off the phase change. If Γ_0 is the initial rate corresponding to pressure p^n at time n, and Δp_0 is the amount of pressure increase which would completely throttle phase change, then

$$p^{n+1} - p^n = [\Delta p_0^{-1} + (\alpha_A + \alpha_B)/c^2 \, \Delta t \, \Gamma_0)]^{-1}$$

would be the result of solving in a completely coupled manner. However, with a fractional step treating cell A in isolation, the sum $\alpha_A + \alpha_B$ in the above expression is replaced by α_A alone. That is, cell A would build up pressure not knowing that the vapor region in cell B is available to relieve the pressure. If $\alpha_A \ll \alpha_B$, the error thus introduced would be substantial. Of course, in the second fractional step in SIMMER, the pressure buildup is relieved by propagation to cell B; this changes

condensation. The impact of such inaccuracies on practical computations has apparently not been studied.

It should be emphasized that the same potential for inaccuracy exists in any fractional step method based on 1-way coupling. The idea is important because fractional step methods have also been used to extend implicit differencing to the fluid convection terms. These fall into the second of the three broad types of finite difference schemes we shall discuss.

6.3. *Fully Implicit Schemes*

For problems where the flow is expected to change only very slowly with time, it may be possible to obtain adequate information from an approximate solution based on very large time steps. This would be advantageous if a reliable and efficient means could be found for solving difference equations treating all terms—exchanges, pressure propagation, and convection—by backward differences. Unfortunately, the state of the art is less satisfactory here than in the case of semi-implicit (convection—explicit) schemes.

It is not surprising that this is the case. Just to backward difference the momentum convection terms would greatly complicate the structure of the difference equations to be solved. Unlike the semi-implicit scheme, there would be no procedure for reducing to a pressure problem by steps which are both local and precise. The fully implicit momentum equations always involve velocities at several nodes, and so cannot be used to eliminate individual velocities. Direct inversion of the fully implicit equations is practical only for 1-dimensional problems. Tractable methods have also been devised under very restrictive assumptions on the flow configuration, such as equal velocities for the phases plus one component of velocity positive at every point [44–48]. (The latter condition is sometimes referred to as parabolic flow.)

Before proceeding, we want to recall that fully implicit schemes are the kind which most clearly show the difference between one and two or three space dimensions. For 1-dimensional problems, one can simply solve the fully implicit difference equations by a global Newton's method with direct inversion of the Jacobian. The direct inversion can be performed by Gaussian elimination, with pivots carefully chosen according to the local direction of flow. If this is done, the computing cost per cell and time stop is roughly twice that of the semi-implicit method. For more than one dimension, direct inversion is not practical, and there is no obvious, affordable inversion method.

To avoid a frontal assault on the problem of solving fully implicit difference schemes, fractional step methods have been tried. The equations can be split into

fractional steps by spatial coordinate or by physical phenomenon, or both. A splitting by spatial coordinate would mean separating

$$S = S_x + S_y, \qquad C = C_x + C_y,$$

where S_x includes all terms which propagate sonic disturbances in the x direction, etc. One might then solve

$$\begin{aligned}(\Delta t^{-1} + E + S_x + C_x)\, w^* &= \Delta t^{-1} w^n \\ (\Delta t^{-1} + E + S_y + C_y)\, w^{n+1} &= (\Delta t^{-1} + E)\, w^* + G.\end{aligned} \tag{6.3.1}$$

The final result is numerically stable provided each step uses a stable scheme; what is not certain is the accuracy of such a scheme. Splitting by spatial coordinates has been tried on many multidimensional partial differential equations, often with the result that accuracy is rather poor for disturbances which propagate skew to the coordinate axes. For two-fluid equations one would expect this problem to be especially severe, since for time steps large enough to justify implicit treatment of convection the sonic coupling across the flow region would be exceedingly strong in all directions. The difficulty is greatest when the flow region is not a rectangle [49]. To our knowledge, spatial splitting is not used for practical two-fluid problems, even though the computational effort to solve successive 1-dimensional steps would be quite reasonable.

All this suggests that a more productive approach would be to split by physical phenomena as well; one of the fractional steps could solve sonic propagation implicitly in all directions, with further steps involving implicit convection terms, possibly split by spatial coordinate. Such a method [38] has been used to overcome the convection limit on time step size in one direction only. This is advantageous if velocities in one (axial) direction are larger than transverse velocities. The method involves two fractional steps, the first a semi-implicit one,

$$(\Delta t^{-1} + E + S)\, w^* = (\Delta t^{-1} - C)\, w^n + G, \tag{6.3.2}$$

where Δt may violate the Lewy condition in the z direction. The second step is an axial stabilizing correction

$$(\Delta t^{-1} + E + S_z + C_z)\, w^{n+1} = (\Delta t^{-1} + E + S_z + C_z)\, w^*, \tag{6.3.3}$$

which, as it turns out, decouples to a set of 1-dimensional fully implicit difference equations. The combined steps are stable if the transverse Lewy condition is respected. This method was shown to be very accurate on a realistic test problem and capable of handling flow recirculation (unlike the parabolic methods). Since the 1-dimensional fully implicit problems consume by themselves somewhat more computing time per mesh cell than the semi-implicit step, this method will be advantageous if the greatest axial velocity is more than twice the greatest transverse velocity.

The 1-dimensional stabilizing correction could be readily augmented by further steps to stabilize the other coordinate directions. This would more than likely yield a fractional step method stable for all time step sizes, but the computational effort per time step would be several times that of the semi-implicit method. This being the case, a 1-step fully implicit scheme may again seem worth attempting. It should also be noted that for multidimensional problems fractional step methods do not converge to a steady state dramatically faster (per unit of computational effort) than the semi-implicit scheme.

Another fractional step method which splits off convection was devised for 1-dimensional problems in [50]. In the shorthand of equations (5.1.3), (5.1.4) it could be described as

$$\begin{aligned}(\Delta t^{-1} + \mathbf{c} + \mathbf{e})\,\mathbf{q}^* &= \Delta t^{-1}\,\mathbf{q}^n - \mathbf{s}r^n + \mathbf{g},\\ (\Delta t^{-1} + \mathbf{e})\,\mathbf{q}^{n+1} + \mathbf{s}r^* &= \Delta t^{-1}\,\mathbf{q}^n - \mathbf{c}\mathbf{q}^* + \mathbf{g},\\ (\Delta t^{-1} + e)\,r^* + s\mathbf{q}^{n+1} &= (\Delta t^{-1} - c)\,r^n + g,\end{aligned} \tag{6.3.4}$$

The first and last steps stabilize convection of momentum and of mass and energy for large Δt; the middle equations constitute a semi-implicit step. This method, christened the stability enhancing 2-step method, is hardly more costly than the semi-implicit method. Although stability conditions have not been proved, it is claimed, on the basis of much experience, that this 2-step method is stable for all Δt, and reasonably accurate for all but a few applications.

It is not hard to imagine generalizing this to more than one space dimension. In fact, such a generalization has been studied [51]. To date, there is unfortunately no description of the results available in the literature.

Finally, let us consider 1-step fully implicit solution of (5.0.1). Substantial efforts have been made to find an efficient method of solving fully implicit difference equations, in particular by Spalding [52]. Equations (5.0.1) are differenced on a staggered grid just as for the semi-implicit method, except that convection-related terms are differenced backwards in time. Spalding's method generalizes a very successful method developed for fully implicit single-phase flow [53].

The two-fluid generalization, like the single fluid method, alternates at each time step between improving the conservation of mass and improving the conservation of momentum. The former is achieved by combining linearized mass conservation equations with the sonic propagation part of the momentum equations, leading to a problem involving pressures only. The resulting pressure problem has, to our knowledge, not been analyzed for its physical content.

Like the semi-implicit scheme, this fully implicit scheme can be iterated, with the fully nonlinear equations used to compute mass and momentum imbalances for the next cycle. However, one fully implicit cycle consists of two separate steps trying to achieve distinct ends, and in practice the iterations do not converge (even for a single phase) unless modified. This is achieved by underrelaxation. In the single phase

computations, only one or two underrelaxation parameters are needed, with good values chosen on the basis of convergence analysis [54]. In the 2-phase case, a greater number of underrelaxation parameters seems advantageous, but there is no supporting convergence analysis. Solutions are obtained by ad hoc experimentation with the underrelaxation parameters. Much experience in this vein has been gathered. Those who urgently need a general, fully implicit solution procedure may want to follow that path.

Another approach is suggested by the single-phase convergence analysis of Wachspress. To paraphase [54], we wish to solve

$$w_t + Cw + Sw = G,$$

or, more specifically,

$$\begin{aligned} r_t + cr + s\mathbf{q} &= 0, \\ \mathbf{q}_t + \mathbf{c}\mathbf{q} + \mathbf{s}r &= \mathbf{g}, \end{aligned} \tag{6.3.5}$$

where $w = (r, \mathbf{q})$ and r stands for either pressure or density (assuming isothermal conditions), while $\mathbf{q}$ stands for the single-phase velocity vector. The implicit difference equations are

$$\begin{aligned} (\Delta t^{-1} + c)\, r^{n+1} + s\mathbf{q}^{n+1} &= \Delta t^{-1} r^n, \\ (\Delta t^{-1} + \mathbf{c})\, \mathbf{q}^{n+1} + \mathbf{s}r^{n+1} &= \Delta t^{-1}\, \mathbf{q}^n + \mathbf{g}. \end{aligned} \tag{6.3.6}$$

To solve these, let estimates $r^*, \mathbf{q}^*$ of $r^{n+1}, \mathbf{q}^{n+1}$ be given, and correct them by amounts $\delta r, \delta\mathbf{q}$ found by solving first

$$\begin{aligned} \Delta t^{-1}\, \delta r + s\, \delta\mathbf{q} &= \Delta t^{-1}(r^n - r^*) + cr^* + s\mathbf{q}^* \\ (\mathbf{d} + \Delta t^{-1})\, \delta\mathbf{q} + \mathbf{s}\, \delta r &= 0. \end{aligned} \tag{6.3.7}$$

(In [54], Δt^{-1} is zero.) This step corrects pressures and velocities to give zero residual in the mass equation, while satisfying an approximate momentum condition. Here $\mathbf{d}$ is the diagonal part of the operator $\mathbf{c}$. This first step gives an elliptic equation for the pressure propagation.

$$[s(\mathbf{d} + \Delta t^{-1})^{-1}\, \mathbf{s} + \Delta t^{-1}]\, \delta r = \cdots.$$

The resulting correction is underrelaxed to give new estimates of r^{n+1}. The $\delta\mathbf{q}$ are not underrelaxed, but are used with the new r^{n+1} in a more complete momentum equation

$$\left(\frac{1}{a}\mathbf{d} - \mathbf{d} + \Delta t^{-1} + \mathbf{c}\right)\mathbf{q}^{n+1} + \mathbf{s}r^{n+1} = \left(\frac{1}{a}\mathbf{d} - \mathbf{d} + \Delta t^{-1}\right)(\mathbf{q}^* + \delta\mathbf{q}) + \mathbf{g}$$

to be solved for $\mathbf{q}^{n+1}$. This equation includes an underrelaxation of the $\mathbf{q}$'s by the factor a. This completes one iteration. Using the new estimates of $r^{n+1}, \mathbf{q}^{n+1}$, we may

return to solve (6.3.7) anew, and so on. Wachspress [54] analyzes the convergence of this process showing that if the underrelaxation factor applied to δr and the a of (6.3.9) are the same, a value slightly less than $\frac{1}{2}$ will give convergence. We note that the same analysis also works if the two underrelaxation parameters are unequal, which appears to be advantageous.

Can this scheme, and the supporting convergence analysis, be generalized to Eqs. (5.0.1)? The appearance of the elliptic problem (6.3.8) suggests they can. We propose the best way to do this is to replace (6.3.7) by the two-fluid sonic propagation problem solved in the semi-implicit method. We can illustrate this merely by changing notation: let r now stand for the two-fluid state vector (p, α, e_1, e_2) and $\mathbf{q}$ for the two-fluid velocity vector. We obtain

$$\begin{aligned} (\Delta t^{-1} + e)\,\delta r + s\,\delta \mathbf{q} &= \cdots, \\ (\Delta t^{-1} + \mathbf{d} + \mathbf{e})\,\delta \mathbf{q} + \mathbf{s}\,\delta r &= 0 \end{aligned} \tag{6.3.10}$$

in place of (6.3.7), or

$$[1 - (\Delta t^{-1} + e)^{-1} s(\Delta t^{-1} + \mathbf{d} + \mathbf{e})^{-1} \mathbf{s}]\,\delta r = \cdots, \tag{6.3.11}$$

which, as we know from Subsection 6.2, is fully equivalent to an elliptic equation representing the effect of sonic propagation with phase coupling. Note that the two-fluid technique of [52] also solves a pressure correction equation similar in appearance to (6.3.8); but it represents pressure propagation neglecting the effect of phase coupling.

By including phase coupling in the pressure correction step (6.3.11) we generalize (6.3.8) to a problem for the generalized r vector which is fully equivalent to an elliptic problem (for p only). We can then hope that the convergence analysis of Wachspress [54] will be applicable. It remains to generalize Eq. (6.3.9) for $\mathbf{q}^{n+1}$ to the dual velocity field, which should be feasible. It would seem preferable to respect the phase coupling here as well. Notice that the iteration steps we propose are quite similar to the fractional steps (6.3.4).

6.4. *Explicit Schemes*

Forward differencing of the terms affecting sonic propagation is certainly appropriate to problems where shocks must be considered, as well as to problems in which disturbances propagate at very high speeds without forming shocks. An example of the former is the particulate-laden rocket exhaust plume [55], while the latter is exemplified by the interior ballistics problem, i.e., the detonation of an artillery charge inside a gun barrel [56]. Large computer codes have been written to study 2-phase flow in each of these applications.

In both applications, the basic finite difference scheme is used in the MacCormack scheme. In the rocket exhaust application, where shock capturing is all-important, the equations are differenced in conservative form. External and internal boundary conditions in both applications are determined with the aid of characteristic

procedures. In the rocket exhaust case this is possible because the dilute particle assumption is used and the equations are hyperbolic. In the interior ballistics applications, the form of Eqs. (5.0.1) is retained in finite differences, that is, the pressure gradient acts on each momentum field in proportion to its volume fraction; but boundary conditions are determined using "pseudo-characteristics" computed as if the pressure gradient were absent from the solid phase momentum equation. Implicit differencing is employed for energy and momentum exchange terms in the interior ballistics problem, to avoid time step limitation due to tight interphase coupling. No mention of implicit exchange terms is made in the description of the rocket exhaust calculation method; presumably the rate constants for exchanges are not so large as to impose limits on the computations.

Another feature of both computer codes is the use of several connected computational zones in which the equations may be simplified in different ways. Such multiple zones are not uncommon in production codes. To date, the specification of different approximations in various zones has usually been done before the computation begins. More flexibility might be achieved if the code could determine the boundaries between zones dynamically as the computation proceeds. Such an approach will undoubtedly come into use if ways can be found to implement it without disproportionate overhead cost.

7.0. *Other Methods*

Although Eulerian finite difference methods are currently the most widely used, other methods do exist. Among them are the method of characteristics, hybrid Eulerian–Lagrangian methods, and weighted residuals.

7.1. *Method of Characteristics*

A few approaches appear unlikely to succeed with Eqs. (5.0.1) at all. The method of characteristics seems to be ruled out entirely because Eqs. (5.0.1) are not hyperbolic. This could be circumvented. By reverting to a 2-pressure equation set, hyperbolic equations can be obtained whose characteristic velocities include those of the corresponding single-phase equations. Whether or not this result is theoretically interesting, it is little consolation in practice. For gas–liquid flow applications, where the single-phase characteristics have at least a microscopic meaning, we know that sound may propagate at a speed much lower than the speed of sound in either phase separately; recall Fig. 4.1. The liquid sound speed plays no role unless the gas is nearly absent. A method of characteristics solution of 2-pressure equations would be most severely constrained by the liquid sound speed, which is usually the feature of least practical interest.

A second instance of circumventing the nonhyperbolicity of Eqs. (5.0.1) occurs in the study of dilute gas-particle flows. In this application it is unclear how one assigns a pressure to the particle field; in practice the pressure gradient in the momentum equations is assigned wholly to the gas phase, and omitted from the particle phase

momentum equations [57]. This appears reasonable since the volume fraction of the gas phase is very close to unity. If this is true, the equations become hyperbolic with characteristic velocities equal to those of the gas phase alone, plus a multiple characteristic velocity in the direction of particle motion. With this form of the equations, the method of characteristics has been applied, for example, to quasi-steady flow of a particle-laden rocket exhaust plume [58]. This steady 2-dimensional problem is equivalent to a transient problem in one space dimension; even in this case, the complexity of shock patterns favors shock capturing techniques, and the use of finite difference methods is growing rapidly.

7.2. *Lagrangian Methods*

Some methods, like the use of stream function or Lagrangian grids, collide head-on with the postulate of two separate fields defined throughout the flow region. Apparently no two-fluid stream function has yet been proposed. A purely Lagrangian method would be cumbersome at best, but there are instances of hybrid Euler–Lagrange finite difference methods in 2-phase flow. One is a generalization of the particle-in-cell (PIC) method [59]. For a problem involving a shock wave in a gas impinging on a fragmented solid, the method substantially reduced numerical diffusion of the shock wave when compared to standard Eulerian finite difference solutions. However, more often in 2-phase flow applications the present state of uncertainty in detailed modelling makes it hard to justify highly accurate solution methods.

Another hybrid scheme which has been highly successful is the PSI-cell method for dilute gas-particle flow [57]. As mentioned above, the equations used are different from (5.0.1) in that the action of the pressure gradient effects the gas phase only. This method iterates between solution of the gas phase flow on a Eulerian grid and integration of the particle state along trajectories. During the particle trajectory calculation, the gas flow is assumed stationary; when the gas flow is recalculated the particle motions are left fixed. Since the particle motion is determined mainly by the gas flow, the method should converge rapidly if the effect of the particles on the gas flow is slight or moderate. Although this method is special to the case of dilute gas-particle flows, it is also in a sense more general than Eqs. (5.0.1), since it can describe, for example, an upward spray in which some particles shoot upward past neighboring ones which are falling back down under the influence of gravity.

The literature on gas-particle flows is extensive; fortunately the recent survey paper by Crowe [57] covers this subject in depth. The hybrid methods developed for dilute gas-particle flow have been extended to gas-particle flows with heavy particle loading [62]; for this difficult problem it is not obvious whether one should prefer hybrid schemes or purely Eulerian methods.

7.3. *Weighted Residuals*

The asymmetric weighted residuals (ASWR) method [60] offers an alternative to finite difference schemes. Similar in spirit to a finite element method, ASWR develops spatial approximation by expanding the solution in a finite-dimensional space of test

functions, and requiring that the differential operator applied to this expansion vanish in a weighted integral sense. The integration weights are chosen from a finite-dimensional weight function space which is different from the space of test functions. If the test functions are denoted by $\{\psi_i\}$ and the weight functions by $\{\phi_j\}$, one seeks

$$w(x, t) = \sum c_i(t)\, \psi_i(x),$$

such that

$$\int [w_t + Ew + Sw + Cw - G] \cdot \phi_j \, dx = 0$$

for each ϕ_j. This method has been implemented for equations like (5.0.1) using a set of test functions made up of linear and quadratic tent-shaped functions at each of the Eulerian nodes and a weight space composed of both characteristic functions of grid intervals and Dirac delta functions. In the test space, a staggered grid is used, so that velocity fields have their test functions centered about grid points which are displaced from the centers of fluid material property test functions.

With the test and weight spaces chosen appropriately, the weighted integrals should give exactly enough conditions to determine the coefficients c_i as solutions of a set of ordinary differential equations; the ODE-solver used for this purpose distinguishes between equations requiring implicit or explicit solution. The method has been applied to a number of 1-dimensional problems, and to multidimensional problems via fractional steps split by spatial coordinate.

The ASWR method is claimed to be more accurate and efficient than finite difference methods for 1-dimensional problems. Discontinuities and shocks can be computed more accurately. The ASWR method is, like the finite difference schemes, subject to the water-packing effect [61], wherein anomalous pressure spikes are computed as a phase boundary moves across an Eulerian mesh cell boundary. This problem has been corrected by introducing discontinuity tracking [63]; although this produces excellent results in one dimension, it is not an approach well-suited to multidimensional problems.

Ultimately, the usefulness of ASWR and other possible higher order methods will be determined by how much accuracy can be justified from the modelling of 2-phase flows.

Appendix 1

The basic model has the form

$$\frac{\partial w}{\partial t} + A \frac{\partial w}{\partial x} = 0.$$

We will show that A has some complex eigenvalues. The most convenient choice for w is

$$w = (p, \alpha, u_1, u_2, S_1, S_2)^T.$$

The equations of state are

$$\rho_i = \rho_i(p, S_i),$$

and

$$(c_i)^{-2} = \frac{\partial \rho_i}{\partial p}.$$

Then the system becomes

$$\begin{aligned}
&(\alpha_2\rho_1 c_1^2 + \alpha_1\rho_2 c_2^2)\,\partial_t p + (\alpha_1\rho_2 c_2^2 u_1 + \alpha_2\rho_1 c_1^2 u_2)\,\partial_x p \\
&\quad + \rho_1\rho_2 c_1^2 c_2^2\,\partial_x(\alpha_1 u_1 + \alpha_2 u_2) = 0, \\
&(\alpha_2\rho_1 c_1^2 + \alpha_1\rho_2 c_2^2)\,\partial_t \alpha + \alpha_1\alpha_2(u_1 - u_2)\,\partial_x p \\
&\quad + \alpha_2\rho_1 c_1^2\,\partial_x(\alpha_1 u_1) - \alpha_1\rho_2 c_2^2\,\partial_x(\alpha_2 u_2) = 0, \\
&\partial_t u_1 + u_1\partial_x u_1 + (1/\rho_1)\,\partial_x p = 0, \\
&\partial_t u_2 + u_2\partial_x u_2 + (1/\rho_2)\,\partial_x p = 0, \\
&\partial_t S_1 + u_1\partial_x S_1 = 0, \\
&\partial_t S_2 + u_2\partial_x S_2 = 0.
\end{aligned}$$

Clearly, two eigenvalues of A (roots of $\det(A - \lambda I) = 0$) are $\lambda = u_1$ and $\lambda = u_2$. It is straightforward to show that the other four satisfy the quartic equation

$$(\phi - \delta)^2\,(\phi + \delta)^2 - \rho_1\alpha_2(\phi - \delta)^2 - \rho_2\alpha_1(\phi + \delta)^2 = 0,$$

where

$$\phi = r^{-1}(\lambda - \tfrac{1}{2}(u_1 + u_2)),$$

$$r = \left(\frac{c_1^2 c_2^2}{\alpha_1\rho_2 c_2^2 + \alpha_2\rho_1 c_1^2}\right)^{1/2},$$

and

$$\delta = (u_1 - u_2)/2r.$$

Let

$$F(\phi) = (\phi - \delta)^2\,(\phi + \delta)^2,$$

$$G(\phi) = \rho_1\alpha_2(\phi - \delta)^2 + \rho_2\alpha_1(\phi + \delta)^2,$$

for real ϕ, $G(\phi) > 0$, $F(\phi) \geqslant 0$, and $F(\delta) = F(-\delta) = 0$.

Since F increases more rapidly than G as $|\phi| \to \infty$, there are always at least two real solutions of $F(\phi) = G(\phi)$, $(\delta \neq 0)$. There will be a multiple real root if there is a real ϕ_0 such that $F'(\phi) = G'(\phi_0)$, $F(\phi_0) = G(\phi_0)$; this occurs if

$$4\delta^2 = |(\rho_1\alpha_2)^{1/3} + (\rho_2\alpha_1)^{1/3}|^3.$$

There are two complex roots if

$$0 < 4\delta^2 < [(\rho_1\alpha_2)^{1/3} + (\rho_2\alpha_1)^{1/3}]^3,$$

or

$$0 < (u_1 - u_2)^2 < \frac{c_1^2 c_2^2}{\rho_2\alpha_1 c_2^2 + \rho_1\alpha_2 c_1^2}[(\rho_1\alpha_2)^{1/3} + (\rho_2\alpha_1)^{1/3}]^3.$$

This result was incorrectly stated in the original version of [34]. The revised version contains the correct expression. A derivation is also given in [18].

REFERENCES

1. M. ISHII, "Thermo-Fluid Dynamic Theory of Two-Phase Flow," Eyrolles, Paris, 1975.
2. D. A. DREW AND L. A. SEGEL, *Stud. Appl. Math.* **50** (1971), 205.
3. R. I. NAGMATULIN, *Intnat. J. Multiphase Flow* **5** (1979), 353.
4. J. R. TRAVIS, F. H. HARLOW, AND A. A. AMSDEN, *Nuclear Sci. Engrg.* **61** (1976), 1.
5. J. H. STUHMILLER, "A Review of the Rational Approach to Two-Phase Flow Modeling," Electric Power Research Institute Report NP-197, 1976.
6. P. P. WEGENER, "Non-Equilibrium Flows I, II" Dekker, New York, 1969.
7. V. H. RANSOM AND M. P. SCOFIELD, "Two-Pressure Hydrodynamic Model for Two-Phase Separated Flow," INEL Report SRD-50-76, 1976.
8. "TRAC PF-1, An Advanced Best Estimate Computer Program for Pressurized Water Reactor Analysis," Los Alamos National Laboratory Report, 1983 (revised).
9. J. HADAMARD, "Lectures on Cauchy's Problem in Linear Partial Differential Equations," Yale Univ. Press, New Haven, Conn., 1923.
10. G. BIRKHOFF AND E. H. ZARANTONELLO, "Jets, Wakes, and Cavities," Academic Press, New York, 1957.
11. D. GIDASPOW, R. W. LYCZKOWSKI, C. W. SOLBRIG, E. D. HUGHES, AND G. A. MORTENSEN, *Amer. Nuclear Soc. Trans.* **17** (1973), 249.
12. J. A. BOURE, "Dynamics des Écoulements Diphasique: Propagation de Petites Perturbations," Commissariat à l'Énergie Atomique Report CEA-R-4456, 1973.
13. P. D. LAX, *Duke Math. J.* **24** (1957), 627.
14. P. D. LAX, *Comm. Pure Appl. Math.* **35** (1980), 395.
15. L. E. PAYNE, "Improperly Posed Problems in Partial Differential Equations," Regional Conference Series in Applied Mathematics No. 22, Society for Industrial and Applied Mathematics, Philadelphia, 1975.
16. P. D. LAX, *Comm. Pure Appl. Math.* **7** (1957), 537.
17. M. ARAI, *Nuclear Sci. Engrg.* **74** (1980), 77.
18. V. H. RANSOM AND D. L. HICKS, *J. Comput. Phys.* **53** (1984), 124.
19. H. B. STEWART, On the mathematics of multifield flow, *J. Math. Anal. Appl.*, to appear.
20. S. L. SOO, *Intnat. J. Multiphase Flow* **3** (1976), 79.
21. B. T. CHAO, W. T. SHA, AND S. L. SOO, *Intnat. J. Multiphase Flow* **4** (1978), 219.
22. L. J. AGEE, S. BANNERJEE, R. B. DUFFEY, AND E. D. HUGHES, Some Aspects of Two-Fluid Models for Two-Phase Flows and Their Numerical Solutions, *in* "Proceedings of the 2nd OECD-NEA Specialists Meeting on Transient Two-Phase Flow, Paris, 1978."
23. M. PLANCK, "Treatise on Thermodynamics," 3rd rev. ed., Dover, New York, 1926.
24. D. A. DREW, Two-Phase Flow, *in* "Multiphase Flow–Proceedings of an ARO Workshop" (J. Chandra and C. K. Zoltani, Ed.), U.S. Army Research Office, 1978.

25. J. H. STUHMILLER, *Intnat. J. Multiphase Flow* **3** (1977), 551.
26. P. S. ANDERSEN, P. ASTRUP, AND O. RATHMANN, "Characteristics of a One-Dimensional Two-Fluid Model for Two-Phase Flow. A Study of Added Mass Effects," RISO (Denmark) Report NORHAV-D-017, 1976.
27. L. VAN WIJNGAARDEN, Some Problems in the Formulation of the Equations for Gas/Liquid Flows, *in* "Theoretical and Applied Mechanics" (W. T. Koiter, Ed.), North-Holland, Amsterdam, 1976.
28. J. D. RAMSHAW AND J. A. TRAPP, *Nuclear Sci. Engrg.* **66** (1978), 93.
29. P. J. O'ROURKE AND F. V. BRACCO, *in* "Proceedings of the Institute of Mechanical Engineers Meeting on Stratified Charge Engines, London, 1980."
30. M. A. GROLMES AND H. K. FAUSKE, *Nuclear Engrg. Des.* **11** (1969), 137.
31. G. B. WALLIS, *Intnat. J. Multiphase Flow* **4** (1978), 585.
32. C. T. CROWE, *Intnat. J. Multiphase Flow* **4** (1978), 255, 231.
33. S. L. SOO, *Intnat. J. Multiphase Flow* **4** (1978), 229.
34. B. WENDROFF, "Two-Fluid Models, A Critical Survey," Los Alamos Scientific Laboratory Report LA-UR-79-291, 1979 (revised).